Quantum Mechanical Calculations of Some Properties of the Crystalline States LiH and LiH:He

by

Shirley W. Harrison

A dissertation submitted to the Graduate Faculty in Physics in partial fulfillment of the requirements for the degree of Doctor of Philosophy, the City University of New York.

1970

This manuscript has been read and accepted by the Graduate Faculty in Physics in satisfaction of the dissertation requirement for the degree of Doctor of Philosophy.

date

Chairman of Examining Committee

date

Executive Officer

Dr. Peter J. Kemmey

Prof. Robert D. Hatcher

Prof. Marvin H. Mittleman

Prof. Raymond L. Disch

Supervisory Committee

The City University of New York

To Roger

May his world be good

Acknowledgments

It is a pleasure to acknowledge Dr. C. Rutherford Fischer's direction and guidance of this study. His contributions to its progress were many and his encouragement and patience were greatly appreciated. I would also like to thank Dr. G. J. Dienes for making available to me the facilities of Brookhaven National Laboratory without which this work could not have been done. During the course of this study, many helpful comments and suggestions were made by a number of people, among them Dr. William D. Wilson, Dr. Peter J. Kemmey and Dr. Ian M. Boswarva. I am also indebted to Dr. Peter Mattern for his assistance in the final stages of the calculations.

This dissertation was made possible in part by a National Aeronautics and Space Administration Traineeship.

Table of Contents

List of Tables

List of Figures

I. Introduction

Lithium hydride in the crystalline state has been the subject of a number of investigations.[1] Various models have been used to calculate crystal parameters, and a number of experimental studies of crystal properties have been made.[2] During the past ten years, the crystalline states LiH and LiH:He have been examined in connection with self-damage due to radiation in mixtures of LiH and its isotopic forms. When these mixtures are stored under conditions varying with factors of time and temperature, this damage results in the formation of helium as well as hydrogen gas and of metallic lithium precipitates. Over long periods of time, volume expansion of the material sufficient to cause crystal fracture can occur.

Quantitative studies of radiation damage were reported by Pretzel and coworkers[3] in 1961, and considerable experimental work has been done since that time[4-6] to determine the exact mechanisms involved. Calculations of the formation and migration energies of a He defect are important in the evaluation of the role of these mechanisms in radiation damage. The results of these calculations can be compared with experimental values[7] of the activation energy for diffusion of He gas in LiH.

The crystal structure of LiH is the same as that of NaCl, i.e., face-centered cubic, and the binding is

considered to be primarily ionic. Point-ion models have been used for ionic crystals with the crystal potential expressed as a sum of a long-range electrostatic potential and a short-range repulsive potential.[8] Parameters in the latter are usually determined empirically from experimental values of crystal properties. Several such models for LiH have been discussed in the literature.[9,10]

Defect calculations for ionic crystals require a model for the host lattice which gives the variation in crystal potential when the ions in the region of the defect are relaxed from the perfect lattice sites. Born-Mayer interactions determined empirically from perfect crystal data have been used for point-ion defect calculations in ionic crystals in which there is no appreciable overlap of charge distributions.[11] This condition is not, however, satisfied in LiH. It is therefore desirable to have a model for the host lattice that takes this overlap of charge into account.

Quantum mechanical calculations of LiH yield a charge distribution for the ions in the crystal. The work of Hylleraas[12] in 1930, which attempts to solve the Schrodinger equation for the entire crystal by the Heitler-London method, is one of the earliest purely quantum mechanical calculations of the properties of ionic crystals. Hylleraas, and later Lundquist,[13] assumed only ionic binding and used screened hydrogenic functions for both the H^- and Li^+ ions. Morita and Takahashi[14] extended

Lundquist's calculations by adding electron-pair or covalent bonding. Hurst,[15] in a calculation of form factors for LiH, used both open- and closed-shell two-electron functions for a single ion and optimized the wave-function parameters in the field of positive and negative point charges arranged to simulate the crystal field.

In discrete models for LiH reported by Fischer et al,[16,17] two-body interactions have been calculated by the Heitler-London method for various wave functions for the H^- ion. Born-Mayer repulsive interactions derived from these calculations have been studied to determine the form of the wave function that leads to a model most consistent with available crystal data. The details of these calculations are discussed in Section II. Crystal parameters obtained are compared with the results found for other models of LiH, including several which have also been used for calculations of He defect properties.[18]

The repulsive interactions determined for the model of LiH have been used in calculating the formation energies for a He defect in the body- and face-centered interstitial positions.[16,19] These calculations are discussed in Section III. The repulsive potentials used for interactions between the defect and the host ions were again based on Heitler-London calculations. The method used in these defect calcu-

lations is that developed by Hatcher and Dienes[20] and extended by Wilson et al.[21] The formation energies are used to calculate an activation energy for He migration which is compared with other calculated values[18,22] and with the experimental results from diffusion studies.[7]

Models for LiH based on pairwise repulsive forces neglect three-body effects shown by Lowdin[1] to be important in ionic crystal calculations. Section IV contains a description of a self-consistent field, molecular-orbital (SCF-MO) calculation of formation energies for the crystalline state LiH:He which attempts to include many-body effects in the region of the defect.[23] Two methods for taking polarization effects into account in this calculation are discussed, one classical and one quantum mechanical.

The polarizability of the ions and the defect in LiH and LiH:He can be related to the corresponding charge distributions in the crystal environment by using the results of previous work by Pauling.[24] A discussion of how the results of the SCF-MO calculations can be used to study these charge distributions is found in Section V. Density contours for the region of the defect are presented. The radial variation of the charge distribution around a given center is used to determine a polarizability for the ion at that location. The variation in polarizability of the ions as they are displaced from the perfect lattice sites by the defect are discussed. Such

variations have been considered[11] to prevent the so-called "polarization catastrophe" in point-ion defect calculations. This phenomenon occurs when the monopole-dipole energy becomes larger than the repulsive energy so that the total energy becomes negative and unbounded as the ions relax.

II. Models for LiH and LiH:He

A. General Formalism

Pairwise interactions between the ions in the crystalline state LiH and between the He atom and the host ions of LiH:He can be calculated using the Heitler-London method. The unsymmetrized wave function for the heteronuclear pair of two-electron systems can be written as

$$\mathcal{K} = a(1)\alpha(1)b(2)\beta(2)c(3)\alpha(3)d(4)\beta(4) \qquad (1)$$

where a, b, c and d are the space parts of one-electron wave functions. From (1), four Slater determinants can be constructed

$$\Psi_1 = |a\alpha b\beta c\alpha d\beta| \qquad \Psi_2 = |a\alpha b\beta c\beta d\alpha|$$

$$\Psi_3 = |a\beta b\alpha c\alpha d\beta| \qquad \Psi_4 = |a\beta b\alpha c\beta d\alpha|$$

For closed-shell systems, a = b and c = d, and the total wave function in the Heitler-London approach is represented by a single determinant. For the open-shell system used in this calculation and discussed in Appendix A, the two-electron wave functions are of the form

$$\mathcal{Q}(1,j) = [a(1)b(j)+a(j)b(1)][\alpha(1)\beta(j)-\alpha(j)\beta(1)] \qquad (2)$$

The total wave function for the heteronuclear pair must be antisymmetric with all exchanges of electrons 1,2,3 and 4, and must vanish when any pair of electrons are in the same state. Thus, as discussed in Appendix A, the total wave function for the open-shell case is given by

$$\Psi = \Psi_1 - \Psi_2 - \Psi_3 + \Psi_4 \qquad (3)$$

This wave function is an eigenfunction of the square of the total spin operator with eigenvalue zero and corresponds to the ground state of the open-shell system.

For a given choice of one-electron wave functions, the total energy of either the open- or closed-shell system for an internuclear separation, R, is given by

$$E(R) = \int \psi^{*} H \psi \, d\tau \qquad (4)$$

where H is the Hamiltonian for the four-electron system. This Hamiltonian contains the electron kinetic-energy operator and the electron-nuclear, electron-electron and nuclear-nuclear potential energy operators and is given in Hartree atomic units) by

$$H = -\tfrac{1}{2}\sum_{i} \nabla_{i}^{2} - \sum_{i,k} \frac{Z_{k}}{r_{ik}} + \sum_{i>j} \frac{1}{r_{ij}} + \frac{Z_{k} Z_{l}}{R} \qquad (5)$$

where r_{ik} is the coordinate of the i-th electron from the nuclear center k and r_{ij} is the distance between two electrons. Z_{k} and Z_{l} are the nuclear charges.

For the single-determinant, antisymmetrized wave function, the energy of (4) is calculated using Lowdin's method for non-orthogonal orbitals.[25] The diagonal matrix element of the electronic Hamiltonian is given by

$$(H)_{av} = \sum (i,j)[i|j] \; \frac{D_{ii}}{\det|S_{pq}|} + \sum_{k>i,l>j} \left\{ [ij|kl] - [il,kj] \right\} \frac{D_{ik,il}}{\det|S_{pq}|} \qquad (6)$$

where S_{pq} is the overlap matrix, with elements given, in

terms of the spin orbitals, u_i, by

$$S_{ij} = \int u_i(1)u_j(1)\, dv_1 \tag{7}$$

and D_{ij} and $D_{ik,jl}$ are determinants formed from $\det|S_{pq}|$ by omitting the rows and columns indicated in the subscripts and including a parity factor.

The integrals with one-electron operators f_1 are written as

$$[i,j] = \int u_i^*(1)f_1u_j(1)\, dv_1 \tag{8}$$

The integrals for the two-electron operator, g_{ij}, are written as

$$[ij,kl] = \iint u_i^*(1)u_j(1)u_k^*(2)u_l(2)g_{12}\, dv_1\, dv_2 \tag{9}$$

For a closed-shell rare-gas diatomic configuration, Slater[26] has shown that the result found from Eq. (6) using the Heitler-London method is equivalent to that found from a molecular orbital calculation. The expression for the open-shell energy of a heteronuclear four-electron system in the Heitler-London approach is derived in Appendix A.

For both the closed- and open-shell cases, the one- and two-center integrals required to calculate the energy at a given value of R are evaluated with the Harwell Laboratory version of the Corbato-Switendick program DIATOM,[27] further modified by Prof. C. R. Fischer for the CDC 6600 computer. No attempt is made in these

energy calculations to apply a variational principle since the interaction energies considered are not the total energies of a physical system.

The repulsive energy for a pair of point ions, or for an ion and the neutral He atom, is found by calculating a net interaction, $E(R) - E(\infty)$, and subtracting any Coulomb energy. Thus the repulsive energy as a function of internuclear separation R is given by

$$E_{rep}(R) = E(R) - E(\infty) - \frac{Q_k Q_l}{R} \qquad (10)$$

where Q_k and Q_l are the net charges on the ions k and l. Curves for the repulsive energy versus internuclear distance are obtained for each interaction with parameters of the one-electron wave functions held fixed.

The repulsive interactions for $Li^+ - H^-$ and $H^- - H^-$ can be represented by Born-Mayer forms. Total energies calculated for $Li^+ - Li^+$ interactions give repulsive forces that are negligible at second-nearest neighbor distances in the face-centered cubic structure of LiH. With six nearest neighbors per ion and six next-nearest H^- neighbors per ion pair, the cohesive energy per ion pair of the fcc LiH crystal is given as a function of R as

$$U(R) = 6A \exp(-BR) + 6C \exp(-\sqrt{2}\, DR) - \alpha \frac{e^2}{R} \qquad (11)$$

where A and B are the Born-Mayer parameters for the $Li^+ - H^-$ interaction, C and D those for the $H^- - H^-$ interaction, α is the Madelung constant for the NaCl structure

(1.747558), and e is the electronic charge.

The equilibrium value of the interionic separation, R_0, can be obtained from the relationship

$$\left.\frac{\partial U}{\partial R}\right|_{R=R_0} = 0 \qquad (12)$$

The cohesive energy of the crystal is obtained from Eq. (11) for $R = R_0$. The compressibility is defined as

$$K = -\frac{1}{V}\frac{\partial V}{\partial P} \qquad (13)$$

where V is the volume per ion pair and P is the pressure. Now

$$\frac{\partial P}{\partial V} = -\frac{\partial^2 U}{\partial V^2} = -\left(\frac{\partial R}{\partial V}\right)^2 \left.\frac{\partial^2 U}{\partial R^2}\right|_{R=R_0} \qquad (14)$$

Since the volume per ion pair in the LiH structure is given by $V = 2R_0^3$

$$\frac{\partial R}{\partial V} = \frac{1}{6R_0^2} \qquad (15)$$

Therefore

$$\begin{aligned}\frac{1}{K} &= V\frac{\partial^2 U}{\partial V^2} \\ &= \frac{1}{18R_0}\left.\frac{\partial^2 U}{\partial R^2}\right|_{R=R_0}\end{aligned} \qquad (16)$$

With the above equations, the cohesive energy, interionic distance and compressibility can be found

for a given wave function for H^-. In empirical determinations of the Born-Mayer parameters, the second term of Eq. (11) is usually omitted and the constants A and B can then be found from Eqs. (12) and (15), using experimental values for R_0 and K. Once A and B are determined, the cohesive energy can be calculated.

B. Numerical Results

The $Li^+ - H^-$ repulsive interaction was calculated for three different types of H^- wave functions with the results shown in Fig. 1. When closed-shell free-ion one-electron wave functions which are close to the Hartree-Fock limit are used for both ions,[28] the curve labeled "Hartree-Fock" was the result. The curve marked "Hurst" is the result of using one-electron hydrogenic wave functions, with parameters found by Hurst,[15] in open-shell wave functions of the form given in Eq. (2). Finally, closed-shell screened hydrogenic functions of the form $\exp(-\delta r)$ were used with an adjustable screening parameter δ for the negative hydrogen ion. The free-ion screening parameter was used for Li^+ since this has been shown by Lundquist[13] and Hurst[15] to be satisfactory for crystal calculations.

Examination of Fig. 1 shows that the Hartree-Fock free-ion H^- function gives the strongest overlap repulsion. This function also leads to the most extended charge distribution for the H^- ion. For the

screened hydrogenic functions, the repulsive energy decreases uniformly as the value of the screening parameter increases, that is, as the charge contracts. The open-shell function, with orbital exponents 1.01 and 0.57 for the one-electron wave functions of the H^- ion, gives results almost identical with the closed-shell function with a screening parameter for the H^- ion of 0.75.

Table I gives the Born-Mayer parameters A and B for Eq. (7), resulting from least-square fits of each of the interactions in Fig. 1 to the exponential forms. The interionic distance and cohesive energy of LiH, considering only first nearest neighbor interactions is also given.

Second neighbor H^- - H^- repulsive interactions are shown in Fig. 2. Some of these interactions are actually attractive. For values of internuclear separation near the interionic distance in LiH, the least contracted wave function yields the most attractive interaction and the most contracted, the most repulsive. This is opposite to the Li^+ - H^- results. For larger values of R, the least contracted function yields the most repulsive interaction. It should be noted that the open-shell function is the only function considered here which includes enough intrashell correlation to yield a bound state for the free H^- ion (E = -0.5133 a.u.). The interaction for this function is repulsive and is again approximately that given by a closed-shell function with δ = 0.75. The repulsive energy in both of these cases

is a linear function of internuclear separation in the region of interest.

The Born-Mayer parameters, C and D in Eq. (11), for the second-nearest-neighbor interactions are given in Table II for various values of the screening parameter. Also given are the corresponding values of interionic distance, cohesive energy and compressibility. The experimental values[29-31] are shown for comparison.

C. Discussion

The attractive interactions for H^- - H^- shown in Fig. 2 are consistent with the results of Hylleraas[12] and Lundquist.[13] Seitz[32] has objected to such an interaction in Hylleraas' calculation, but the present calculations confirm the fact that closed-shell models for two-electron systems can yield such results.

As can be seen from Table II, however, the best fit to crystal data is found for the H^- screened hydrogenic wave functions which give repulsive interactions and result in a considerable contraction of the charge distribution as compared to the free ion. This contraction is in general agreement with the results of Lundquist[13] and Hurst.[15] The free-ion Hartree-Fock function for H^- leads to an attractive H^- - H^- interaction and a charge distribution which is much too extended to yield a reasonable model for LiH according to the methods used here.

The strongest H^- - H^- interaction changes the value of R_0 and U by only six percent compared to those for

first nearest neighbors only. The values are still high compared to the experimental values. The compressibility values for large screening parameters are low compared to reported experimental values.[30, 31] Subhadra and Sirdeshmukh[33] have analysed the experimental data for the compressibility of LiH and find that the use of the reported values with a simple Born-Mayer model of LiH leads to elastic constants which violate the Born conditions for crystal lattice stability.[34] They conclude that the measured values are in error and predict an upper bound of 2.15×10^{-12} cm^2/dyne. Recent work of Wilson and Johnson[18] attributes the disagreement between theory and experiment to the assumption of only central forces in the discrete lattice theory.

LiH crystal parameters calculated by other investigators are presented in Table III. Lundquist[13] found upper and lower limits of -8.45 and -8.77 eV/ion pair for the cohesive energy of LiH by applying a molecular orbital method to the entire crystal. Screened hydrogenic functions with free-ion parameters were used for the H^- and Li^+ ions. For the same functions in the pairwise interaction model, the cohesive energy is -8.39 eV/ion pair (Table I). The neglect of three-body forces in the pairwise interaction model could account for the difference in energy. Model I of Wilson and Johnson,[18] which includes the effect of non-central forces for first and second nearest neighbors, gives a cohesive energy of -8.50 eV/pair. Model II, which includes the effect of these forces for only first nearest neighbors, gives a co-

hesive energy of -8.10 eV/pair.

With Hurst's open-shell crystalline H^- function, the cohesive energy obtained in the diatomic calculation differs from Hurst's result using the same function by almost twenty percent. This difference may be due to the fact that Hurst carried out his calculation at the experimental value of the interionic distance rather than at an equilibrium value appropriate to his model. His model also neglects antisymmetrization effects which are partly included in the diatomic calculation.

In the diatomic calculation, the large value of the H^- screening parameter required for best fit to crystal data (0.90 as compared to 0.6875 for the free ion) corresponds to the redistribution of charge of this ion that would arise from a properly symmetrized wave function[35] and also takes into account, as mentioned previously, the contraction of the H^- ion in the crystal field. The first of these effects is included in Lundquist's calculation, which could account for the much smaller change in screening constant (from 0.6875 to 0.7208) required in his case to obtain the best fit to the data.

The open-shell configuration leads to a charge distribution for the crystalline H^- which differs markedly from the distribution obtained from the screened hydrogenic function with $\delta = 0.75$, yet both the $Li^+ - H^-$ and $H^- - H^-$ repulsive interactions obtained with the two different wave functions are almost identical. This result suggests that

the finer details of ionic charge distributions may not be of such importance when two-body repulsive interactions are being calculated, and that closed-shell screened hydrogenic functions may be adequate for this purpose. This type of result has been obtained previously. For example, Thomas-Fermi type of charge distributions yield interactions in various diatomic calculations almost identical to those found from single or even multiconfiguration MO-SCF calculations.[36]

The diatomic calculations as related to the LiH crystal data provide a basis for calculating interaction energies between a He defect and the ions of the host lattice. The changes in interaction energies in the host lattice resulting from relaxations of ions around the defect can also be evaluated. Parameters for a repulsive interaction obtained from a theoretical calculation of interactions over a range of internuclear distances should be more reliable than those obtained from crystal data relating to a single interionic distance.

III. Point-ion Defect Calculations

A. Method

When a point defect is present in a crystal, the ions in the region surrounding the defect are relaxed from their positions in the prefect crystal. For a fixed position of the defect, the relaxations corresponding to a minimum in formation energy (total energy of the defect state relative to the pure state) are found by assigning variable displacement parameters to ions surrounding the defect and minimizing the formation energy with respect to these parameters.

Following the method developed by Hatcher and Dienes,[20] and extended by Wilson et al,[21] the formation energy for a defect state is expressed as a sum of changes in electrostatic, repulsive and polarization energies. The electrostatic energy change is a correction to the Madelung energy of the perfect crystal due to relaxations of the lattice ions, plus an additional electrostatic energy if the defect is charged. The change in repulsive energy is calculated using the Born-Mayer parameters determined from the calculations of two-body interactions for ions in the host lattice. The additional repulsive energy between the host lattice ions and the defect is also included. Repulsive interaction energies up to third nearest neighbors are taken into account.

In the perfect crystal the electric field at each point ion vanishes by symmetry and hence polarization energy is zero. With the defect present, the relaxations of the ions create a non-zero electric field at the ion sites

which gives rise to induced dipoles and associated dipole fields. The polarization energy is given by

$$E_{pol} = -\tfrac{1}{2} \sum \vec{p}_i \cdot \vec{E}_i^{chg} \qquad (17)$$

where the sum is over all polarizable ions, $\vec{p}_i$ is the induced electronic dipole moment on ion i due to the field of the charges and dipoles surrounding it, and $\vec{E}_i^{chg}$ is the monopole electric field at ion i due to the asymmetrical distribution of charges surrounding it. The value of the dipole moment for ion i, p_i, is written in terms of the monopole field and the dipole field as

$$\vec{p}_i = \alpha_i \vec{E}_i^{chg} + \alpha_i \sum_{j \neq i} \left\{ \frac{3\vec{r}_{ij} \cdot \vec{r}_{ij} - \vec{\vec{I}} |\vec{r}_{ij}|^2}{|\vec{r}_{ij}|^5} \right\} \vec{p}_j \qquad (18)$$

where α_i is the polarizability of ion i, $\vec{r}_{ij}$ is the position vector of ion j relative to ion i in their relaxed configuration, and $\vec{\vec{I}}$ is the unit dyadic. Thus for a given number of dipoles a set of simultaneous equations must be solved to calculate the polarization energy.

In the solution of these equations, the α are assumed to be known. For some ionic crystals, the free-ion polarizabilities of the constituent ions can be used.[37] The polarizability of the free H^- ion has not been uniquely determined.[38] Moreover, values for the free-ion do not apply since the H^- ion is contracted in the LiH crystal. An estimate of α can be obtained from the Lorentz-Lorentz relation for the NaCl structure

$$\frac{n^2 - 1}{n^2 + 1} = \frac{2}{3R_0^3} (\alpha_+ + \alpha_-) \qquad (19)$$

where n is the refractive index and α_+ and α_- are the cation and anion polarizabilities. If the free-ion value for Li^+ is used in this formula, a value for H^- can be found.

Since the ions in LiH are of very different sizes, the central dipole approximation, which leads to a constant polarizability, is not strictly satisfied. The H^- polarizability determined from ionic or pure crystal data for LiH may therefore need to be further adjusted or varied.[11]

B. Results

In a calculation previously reported,[16] a point-ion defect model based on the repulsive interactions determined for the pure crystal was used to calculate activation energy for He migration in LiH. The cube-centered interstitial position was assumed to be the most stable for the neutral defect, with migration taking place through the center of an adjacent face. The activation energy is the energy needed to move the defect across the potential barrier between positions of stable equilibrium. It is therefore given by the difference of formation energies for the face-centered and the body-centered positions of the defect.

The change in repulsive energy due to relaxations of the host ions was calculated using Born-Mayer parameters for first-nearest neighbors corresponding to a screening parameter of 0.95 for the H^- ion (Table I). The parameters used for second-nearest neighbor H^- interactions were A = 5.0510 eV/ion pair and B = 2.0859 Å^{-1}. These values correspond to a screening parameter between 0.72 and 0.75.

In this model the charge distribution of the H^- ion is more extended toward a like ion than toward the neighboring Li^+.

The parameters for the He-Li^+ repulsive interactions determined by the method described in IIA were A = 615.99 eV/pair and B = 5.0680 Å^{-1}. For the He - H^- interaction, two values of the H^- screening parameter were considered and the resulting values of the activation energy compared.

The polarizability of Li^+ (0.029 Å^3) was taken from Tessman, Kahn and Shockley[37] and that of He (0.203 Å^3) from Pauling.[24] Equation (19) with a value for n = 1.984 taken from Pretzel et al[3] gives α = 1.93 Å^3 for the crystalline H^- ion. This is consistent with the contracted wave function for H^- and Pauling's relationship between α and δ,[24] which for two-electron systems becomes

$$\alpha = \frac{1.34}{\delta^4} \qquad (20)$$

However, with the repulsive interactions used in this preliminary calculation, this value of polarizability resulted in an unstable defect model and a lower value had to be used. For α = 1.00 Å^3, the activation energy for He migration was found to be 0.27 eV and 0.25 eV, respectively, for δ = 0.7208 and 0.95 in the He - H^- interaction.

For these models, the volume expansion of the lattice per He defect, estimated from first nearest neighbor displacements for the body-centered position, was between 5.0 and 5.6 Å^3.

A later calculation[19] of the activation energy for He

in LiH employed the two-body $Li^+ - H^-$ interactions for $\zeta = 0.90$ and used an $He - H^-$ interaction determined from a generalization of the semiclassical method of Wedepohl[39] for treating interactions between like ions. In this calculation the polarizability of the H^- ion was assumed to decrease with distance from the ions near it to prevent polarization catastrophe. A value of 1.93 $Å^3$ was assumed at $R = R_0$. This gave a stable defect model with an activation energy of 0.6 eV for He migration from a body-centered stable position through an adjacent face. The volume expansion per He defect was estimated to be between 7 and 8 $Å^3$.

C. Discussion

The activation energies calculated from the point-ion model can be compared with values reported by other workers for discrete models. Jaswal and coworkers used a deformation dipole model to determine the dynamical matrix of the LiH lattice,[40] making use of experimental phonon dispersion curves. In calculations of the activation energy of a He defect, the potential energy of the distorted crystal was treated in the harmonic approximation. An early calculation[22] used a defect host-ion interaction of the Huggins-Mayer form with the parameters computed from a known He - He potential. The migration energy reported was 0.8 eV. In later calculations,[41,42] the Heitler-London method was used with a Slater orbital for H^- ($\zeta = 1.0$) expanded ten Gaussians (exponentials with an r^2 variation rather than an r variation as in screened hydrogenic functions). Defect calculations using these inter-

actions gave a migration energy of 0.65 eV.

Wilson and Johnson,[18] using the repulsive interactions described in II together with a variable polarizability for H^-, found migration energy values of 0.69 and 0.87 eV for the two different sets of crystal parameters for LiH given in Table III.

These calculated values can be compared with experimental results. Jones[6] has estimated an activation energy of 0.4 eV based on the size and separation of He bubbles in damaged LiH:LiT. More recently, a high-temperature result of 1.22 eV for the activation energy of diffusion of He gas in crystalline LiH has been reported.[7] The difference between this measured value and calculated values has been attributed[18,41] to trapping of significant fractions of the He gas in intrinsic defects.

Experimently observed volume expansion in mixtures of LiH and LiT vary with storage conditions of temperature and time. On the basis of experimental results and the half-life of T^-, Pretzel and Petty[4] have estimated the low-temperature (below 0°C) expansion due to interstitial He to be 12.4 A^3/β decay. Because of the lack of agreement between calculated and observed values, other mechanisms for low-temperature expansion in LiH:LiT have been examined.[19]

IV. Many-Body Calculations

A. Method

To investigate such questions as many-body forces, charge distributions and the polarizability of ions, a molecular-orbital (MO) method, modified to include the crystal environment, can be used to find approximate solutions of the Schrodinger equation for the defect region of LiH:He. Electronic structure is associated with the defect and with a group of neighboring ions, and this structured group is surrounded by a sufficient number of point ions to simulate the crystal field in the neighborhood of the structured ions. Following the method of Roothaan[43] the molecular orbitals are formed from linear combinations of a basis set of N atomic orbitals (LCAO). Thus

$$\Phi_r = \sum_{i=1}^{N} Y_{ri}\eta_i \qquad (21)$$

where η_i are the basis functions and Y_{ri} the normalized coefficients of these functions in the molecular orbital.

On the basis of the study of the point-ion model of the perfect crystal, closed-shell atomic orbitals can be used for both the H^- and Li^+ ions. The He defect is also a two-electron, closed-shell system. For a closed-shell system, the total wave function for the defect region is a single determinant of doubly occupied molecular orbitals

$$\Psi = \frac{1}{\sqrt{(2M)!}} \det\left|\Phi_1(1)\alpha(1)\Phi_1(2)\beta(2) \cdots \right. \\ \left. \cdots \Phi_M(2M-1)\alpha(2M-1)\Phi_M(2M)\beta(2M)\right| \qquad (22)$$

where M is the number of structured centers in the model of a given crystalline defect state of LiH:He. An approximate solution of the self-consistent field (SCF) problem is found by minimizing the total energy of the semi-discrete model of the defect state with respect to the coefficients Y_{ri} of the atomic orbitals. The details of this calculation are discussed in Appendix B. The total energy of an equivalent model of the perfect crystal is also calculated by the LCAO-MO-SCF method and subtracted from the total energy of the defect state to find the change in energy due to the addition of the defect. The formation energy is found by subtracting the self-energy of the defect from this change in total energy.

In the molecular-orbital calculations, all ions surrounding an ion that is allowed to relax in the presence of a defect must be structured since the amount of overlap determines the change in repulsive energy. In this calculation only the first nearest neighbors to the defect are allowed to relax since the point-ion model shows these relaxations to be large compared to those of ions further from the defect. The minimum in formation energy is found by varying these relaxations.

The two-electron integrals needed to calculate the total energy involve as many as four centers. Also, the total number of distinct one-electron integrals to be evaluated varies approximately as $N^2/2$ and the total of two-electron integrals as approximately $N^4/8$, where N is the

number of atomic orbitals used to form the molecular orbitals. For a basis set of 50 functions, which is about the number required in this problem, there are 1275 distinct one-electron integrals and 814,725 two-electron integrals.

Serious computational difficulties arise in evaluating these integrals if screened hydrogenic functions are used. To avoid these difficulties in studying complex molecules, a number of investigators in quantum chemistry[44] have made use of Gaussian functions. For s- and p-symmetry types, these are of the form

$$\eta = (C_s + C_x X + C_y Y + C_z Z) \exp(-\alpha r^2)$$

The dependence of this function on r^2 rather than r avoids the appearance of square roots in expressions involving functions of different distances. Also, Gaussians have the property that products of functions centered on different origins are proportional to a single Gaussian with a center on the line joining the origins of the product functions. For these reasons, nearly all of the integrals in the molecular orbital calculation can be evaluated analytically. For the most difficult type, a single numerical integration is required.

The evaluation of the integrals and the SCF calculation can be carried out on the CDC 6600 with a modified version of POLYATOM.[44] The details of the program are discussed in Appendix B. Symmetry properties of the structured group of ions are introduced to reduce the number of unique integrals and symmetry orbitals which are irreducible represen-

tations of the symmetry group are used to simplify the SCF calculations.

Gaussian functions have been used in calculations of the LiH molecule[45] and for calculating the energy of the He atom.[46] The results obtained for single atoms and for simple molecules show that more Gaussian than Slater functions are needed for calculation of primary properties. There is evidence, however, that reliable values for energy differences can be obtained with a limited set of Gaussian basis functions.[47] Since equivalent sets of lattice ions are structured in the two LCAO-MO-SCF calculations (with and without the defect) relatively few Gaussians are associated with the individual ions. For the defect, which appears in only one part of the calculation, a more extended set of atomic orbitals is used. The self-energy of the defect used in calculating the formation energy of a defect state is that corresponding to the basis set used.

A check on the reliability of the values found for energy differences, with a limited set of Gaussians, can be made by using the virial theorem.[48] This theorem implies that in going from one stable configuration to another the changes in kinetic energy and potential energy satisfy the relationship

$$\Delta T = -\tfrac{1}{2}\Delta V$$

For the defect problem, this relationship should hold at the minimum value of formation energy.

Polarization energy is taken into account to some

extent in an LCAO-MO-SCF calculation that includes Gaussians with only s-type symmetry. There is a limited amount of distortion of the charge distribution surrounding the ions that relax due to the lack of symmetry. Polarization energy can be further taken into account by including p-type Gaussians in the basis set of atomic orbitals to give more flexibility in the wave function. For comparison purposes, a polarization energy can be calculated separately in the classical point-ion model.

B. Description of Calculations

The optimum value for a single Gaussian to approximate a single Slater-type orbital can be calculated as shown by Huzinaga[46] from

$$\zeta = (Z')^2 \alpha_{opt} \qquad (23)$$

where ζ is the coefficient in the exponent of the Gaussian orbital, Z' is the screening parameter for the Slater orbital and α_{opt} is a constant depending on the symmetry of the orbital. For a 1s orbital, $\alpha_{opt} = 0.2829$. Thus the three optimum values of interest for the LiH:He problem are

	Z'	ζ
H^-	0.6875	0.1337
He	1.6875	0.8057
Li^+	2.6875	2.0433

For He, Huzinaga has calculated the orbital parameters for N gaussians with N = 2 to 10. The values for N = 2 were

used to obtain parameters for two Gaussians for an H^- or Li^+ ion by using simple ratios to the optimum single values in each case. The set of orbital parameters used for various ions in the defect region are shown in Table IV along with Huzinaga's values for He for N = 2 and 9.

The cube-centered interstitial position is assumed to be the most stable for a neutral He defect in this model for LiH:He. Migration of the defect between positions of stable equilibrium was again assumed to take place through the center of the cube face. The activation energy is the energy needed to move the He across the barrier between positions of equilibrium.

The minimum total energy for the cube-centered position of the defect was determined by varying the relaxations of the eight nearest neighbors at the corners of the cube shown in Fig. 3. As indicated at one corner of the cube, each nearest neighbor has three neighbors which are nearest to it and which are second-nearest neighbors to the defect. Thirteen more groups of n-th order neighbors with n = 3 to 15 were included as point ions so that all ions within $\sqrt{30}$ times the interionic distance from the defect were included. This gave a total of 673 centers for the defect region in the model of the body-centered case.

The relaxations were assumed to be radial from the defect, the ions moving along the body diagonal of the cube. The H^- ions are more diffuse than the Li^+ ions so that the overlap will be greater for He - H^-. On the basis of results obtained with the point-ion model, is was assumed

that the relaxations for H^- were greater than for Li^+. The experimental value of the interionic distance in LiH, 3.86 a.u., was used.

In calculating the minimum total energy for a face-centered interstitial He defect, the four nearest neighbors to the defect were allowed to relax. Fig, 4 shows the ions at one corner of the face which were structured for the LCAO-MO-SCF calculation. All nearest neighbors of the ions that are allowed to relax are structured. This gives equivalent conditions to those used in the body-centered defect calculations. A fifth nearest neighbor to the defect and one of the second nearest neighbors to the ion that is allowed to relax was also structured since the latter moves radially outward toward the former. The equivalent ion in the body-centered was assumed to be a point ion since it is a third nearest neighbor to the ion that is allowed to relax and is a body diagonal away. The face-centered defect model thus includes structure for a total of 25 centers counting the defect. The effect on the formation energy of the choice of ions structured was studied for this case by varying the number to include only nearest neighbors to the ions that are relaxed in one case and all second-nearest neighbors to the ions that are relaxed in another case. Point ions up to $\sqrt{30}$ times the interionic distance were again included in all calculations, giving a total of 681 centers for the face-centered case.

As noted in IV-A, the total number of integrals that

must be evaluated in the molecular orbital approach can be reduced by taking into account the symmetry of the group of structured ions. As can be seen from Fig. 3, the body-centered group has three axes of rotational symmetry, the three rotations belonging to the group D_2 which has four irreducible representations. The face-centered configuration, Fig. 4, also has three axes of rotational symmetry, and in addition three planes of reflection and a center of inversion. The transformation group is D_{2h} and there are eight irreducible representations.

Some p-type Gaussians were included in one set of calculations for a face-centered defect. Two p_x, p_y and p_z Gaussian orbitals with parameters taken from Csizamadia[45] were added to the basis set for nearest neighbors only. If two of the coordinates are chosen along the face diagonals, the same transformation group can be used.

C. Results

Curve I in Fig. 5 shows the formation energy in Hartree atomic units versus nearest-neighbor relaxation for the body-centered He defect. The basis set of atomic orbitals is limited to Gaussians of s-type symmetry. The relaxation parameter P_1 is that associated with the H^- ion and the radial relaxation is given by P_1 times the interionic distance in the perfect crystal. A similar parameter P_2 is associated with the Li^+ ion. On the basis of point-ion defect calculations, it was assumed that $P_2 - P_1 = 0.01$ for all values of P_1.

The energy of the He defect used in calculating the formation energy was that given by Huzinaga[46] for the nine orbital parameters in Table IV. This energy is -2.86165 a.u. as compared to the Hartree-Fock value of -2.86168 a.u.

Curve II in Fig. 5 gives the polarization energy as computed from the point-ion defect model, allowing only nearest-neighbor relaxations and assuming these to be the same as those used to obtain Curve I. The polarizability of the H^- ion was assumed to be constant and to be equal to 1.93.

Curve III was obtained by adding curves I and II. This causes the minimum formation energy to be shifted down from 0.045 a.u. (1.21 eV) to 0.030 a.u. (0.82 eV) and to the right, from $P_1 = 0.075$ to $P_1 = 0.14$.

Fig. 6 shows a similar set of curves for the face-centered defect with the basis set in the LCAO-MO-SCF calculation again limited to s-type Gaussians. Based on the point-ion defect calculations, it was assumed in this case that $P_2 - P_1 = 0.16$ for all values of P_1. The minimum for Curve I is at $P_1 = 0.20$ with a formation energy of 0.061 a.u. or 1.64 eV. The minimum for the corrected curve is at $P_1 = 0.24$ with a formation energy of 0.035 a.u. or 0.95 eV. These results are for 25 structured centers, as discussed in IV-B.

If only first nearest neighbors to the ions that relax are included, there are 21 structured centers. If all second-nearest neighbors are included, the total number of centers is 41. The variation in formation energy (no correc-

tion for polarization energy) with number of centers for $P_1 = 0.22$ is as follows:

No. of Centers	Formation Energy	
21	0.077 a.u.	2.07 eV
25	0.063	1.64
41	0.043	1.21

The activation energy calculated from the LCAO-MO-SCF formation energies (minimums of Curves I in Figs. 5 and 6) is 0.016 a.u. or 0.43 eV. Use of the formation energy for 21 centers in the face-centered case would increase this value to about 0.020 a.u. or 0.54 eV. With the correction for polarization energy, the activation energy of 0.43 eV would be reduced to 0.14 eV. All of these values are low compared to the most recent values found for point-ion models (see III-C).

Fig. 7 shows the formation energy versus relaxation of the H^- ions for the face-centered case calculated with and without p-type Gaussians. For the curve labeled II, these functions were used only on H^- nearest neighbors. The point labeled IV was calculated with p-type Gaussians on all four nearest neighbors to the defect. Because the total number of functions needed increases rapidly when p-type functions are added (six on each center) only two s-type functions were used for the He defect. Curve I in Fig. 7, which shows the formation energy versus relaxation without p-type Gaussians, is higher by a constant amount as compared

with Curve I in Fig. 6, because of the difference in size of the basis set for the He defect. The energy of the He atom calculated with only two Gaussian orbitals is -2.7407 a.u. as compared to -2.8616 a.u. for nine orbitals.

The effect of including the p-type Gaussians in the LCAO-MO-SCF calculations is to shift the curve for formation energy down and over in the same manner as with the correction from the point-ion calculation of polarization energy (Curve III of Fig. 6). Not all of the change in energy between curves I and II in Fig. 7 can be attributed to polarization energy since the repulsive (overlap) energy will be different for the two basis sets. Because of limitations of machine time, no defect calculations for the body-centered case with p-type functions were carried out.

Table V shows the total kinetic and potential energies at the minimum of formation energy for the face- and body-centered positions with s-type basis functions and for the face-centered position with p-type functions added. It can be seen that the virial theorem is well satisfied for the differences in energies in all cases even though it is not satisfied for the total energies. The latter have no physical meaning in this calculation since the energy between point ions surrounding the structured ions does not include any electronic part.

V. Charge Density Distribution and Polarizability

A. Theory

The LCAO-MO-SCF calculations described in IV-A lead to analytic expressions for the occupied molecular orbitals, ϕ_r, in the many-body models of LiH and LiH:He. These expressions contain the Gaussian functions η_i and the values of the variable coefficients Y_{ri} corresponding to the minimum value of the total energy in the SCF calculation. At a given point in a particular model, the charge density (probability density) for each molecular orbital is given by

$$\rho_r = 2|\phi_r|^2 = 2\sum_{i=1}^{N}\sum_{j=1}^{N} Y_{ri}Y_{rj}\eta_i\eta_j \qquad (24)$$

Since the moecular orbitals correspond to irreducible representations of a symmetry group, they are orthogonal and the total charge density at any point is given by

$$\rho(r) = |\Psi|^2 = \sum_{r=1}^{M}\rho_r \qquad (25)$$

The Y_{ri} values are given as part of the output data of POLYATOM (see Appendix B). These values are then used to calculate the orbital and total charge densities at any point in the three-dimensional model. These calculations were carried out on the CDC 6600 using the program DENPLOT.[49] With this program, densities in a specified plane can be used to display density contours as part of the printed output or on a cathode-ray tube for a 35mm film record.

The DENPLOT program can also be adapted to give total

charge density as a function of distance from a given center in the model. Total charge in a finite region around a given center is found by calculating the radial distribution function

$$D(r) = \rho(r)r^2 \qquad (26)$$

and integrating this function as far as necessary to give a value close to unity. The maximum value of D(r) determines a most probable radius for a given ion for a given basis set.

Charge density distributions corresponding to single Slater screened hydrogenic functions can be fitted to the charge density distributions obtained with the Gaussian set of atomic orbitals in the vicinity of a given center. The method of least squares can be used with the hydrogen screening parameter ζ as a variable and with the hydrogenic function normalized to give unit charge when integrated over all space. The screening parameters found in this way can be used to determine polarizabilities of the ions in the crystal, using Pauling's expression for ζ for electrons moving in a pure Coulomb field.[23] For two-electron systems with a single closed shell, the relationship as given in Eq. (20) is

$$\alpha = \frac{1.34}{\zeta^4}$$

where α is in Å^3. If α is determined for the Li^+ or H^- ions for various relaxed positions, polarizability as a function of displacement can be studied.

B. Charge Density Contours

The effect of a face-centered interstitial He atom on the charge distribution of the ions in LiH was studied by using the molecular orbital coefficients obtained in the calculations of formation energy versus displacement of the H^- ion (Curve I of Fig. 6). Densities in the plane containing the defect and its nearest neighbors (see Fig. 4) were calculated to determine charge distributions around 16 ions near the defect, which is located at the origin when present. The eight second-nearest neighbors to the defect lie in two planes parallel to this plane and separated from it by plus and minus the interionic distance. For the LiH:He state, the displacements of nearest neighbors to the defect take place in the plane for which the charge densities have been calculated.

For the perfect crystal model the maximum density in the plane, found by summing all 24 orbitals, is 3.50 $(a.u.)^{-3}$ and occurs at the center of the Li^+ ion. The total density at the center of the H^- ion is 0.092 $(a.u.)^{-3}$ or only about three percent of the Li^+ maximum. The scale of intensities on the screen of the cathode-ray tube in the CALCOMP plotter associated with the CDC 6600 corresponds to a range of densities from maximum to one percent of maximum. For this reason, very little structure for the H^- ion would be observed if the total density from all 24 orbitals was displayed. Therefore, densities from those orbitals with large coefficients for the H^- atomic orbitals were added to display

density contours in the vicinity of these ions. These contours are shown in Fig. 8. The structure of the Li^+ ions, obtained by adding the remaining orbitals, is shown in Fig. 9. Since both plots cover the same area of the plane, it can be seen that the charge is much more concentrated around the Li^+ ions. It should be noted that the four-leaf clover pattern in these pictures is a result of the method of plotting. Checks of numerical values show that it has no significance as far as the symmetries of the electron density contours are concerned.

The twelve orbitals used for Fig. 9 are the first twelve in order of increasing orbital energy. The maximum density for the sum of these orbitals is 3.45 $(a.u.)^{-3}$, showing that there is a small contribution to the charge density around the Li^+ centers of the remaining twelve orbitals. This can also be seen in Fig. 8. The maximum density for the twelve orbitals used for the H^- contour plots (Fig. 8) is 0.092 $(a.u.)^{-3}$, showing a negligible contribution from the twelve Li^+ orbitals. This can also be seen from Fig. 9 which includes densities as low as 0.035 $(a.u.)^{-3}$ but shows no contours around the H^- ion sites.

The two lowest orbital energies for LiH are -2.387 and -2.385 a.u. as compared to an orbital energy of -2.680 for a free Li^+ ion with a wave function made up of a linear combination of the two Gaussian atomic orbitals associated with the Li^+ in the crystal calculation. The density contours for the orbital with the lowest orbital energy is

shown in Fig. 10. This orbital has significant charge density only on the two Li^+ ions nearest the origin (nearest neighbors to the defect site). The maximum density is about half that of Fig. 9, the total charge in this orbital being equally divided between the two Li^+ ions. Thus the four most tightly bound electrons can be said to be the 1s electrons of these two ions.

With the He defect at the origin (face-centered position) of the group of structured ions, there are 25 molecular orbitals. In order of increasing orbital energy, the thirteenth orbital has the largest coefficients for the nine He atomic orbitals, and an orbital energy of -1.1095 a.u. as compared to -0.9179 a.u. for a free He atom using the nine Gaussian atomic orbitals. The latter is equal to the Hartree-Fock value. The coefficients for the nine Gaussian functions for the crystal orbital and for the free He atom are given in Table VI and can be seen to be very similar for the two cases.

The density contours for this orbital are shown in Fig. 11. The maximum density is 1.63 $(a.u.)^{-3}$ as compared to a total density, found from summing all 25 orbitals, of 1.81 $(a.u.)^{-3}$ so that there is about a ten percent contribution from the other 24 orbitals. Allowing for the difference in scale between Figs. 10 and 11, the charge density around the He falls off more slowly than that of the Li^+ ion.

The He orbital was included with the twelve Li^+ orbitals (first in order of increasing orbital energy) in com-

puting the charge density contours around the Li^+ ions with the defect present. Fig. 12 shows this charge distribution for the relaxation of the nearest neighbor ions which gives a minimum of formation energy for the face-centered interstitial He, i.e., $P_1 = 0.20$ in Fig. 6. Since Fig. 12 shows densities down to one percent of maximum for the Li^+ ions, which corresponds to only 30 percent of the maximum for the charge density of the He defect, the difference in extent of the Li^+ ion and the neutral He defect is not apparent.

Comparison of Fig. 12 with Fig. 9 shows very little change in the Li^+ charge distribution with and without the defect. The maximum density in Fig. 12 is slightly lower than that in Fig. 9, but if the densities of all 25 orbitals are added, the maximum density at the nearest neighbor Li^+ is 3.49 $(a.u.)^{-3}$ at the relaxed position as compared to 3.50 $(a.u.)^{-3}$ for the no defect case.

The density contours for the sum of the twelve remaining orbitals for $P_1 = 0.20$ are shown in Fig. 13. The contribution of these orbitals to the charge density of the Li^+ ion is again apparent, as is the contribution to the charge density around the He defect. The contours around the nearest neighbor H^- ions in Fig. 13 appear to be slightly distorted. This distortion is even more noticeable in the density contours for the most loosely bound electrons, shown in Fig. 14. However, if all 25 orbitals are added and the density variations along various directions are compared, there is no significant difference.

The increase in the maximum density, 0.0967 (a.u.)$^{-3}$ in Fig. 13 as compared to 0.0917 (a.u.)$^{-3}$ in Fig. 8, is an indication of a more contracted H^- ion. Densities found in summing all 25 orbitals show an increase in the maximum density at the nearest neighbor H^- ion from 0.092 (a.u.)$^{-3}$ to 0.107 (a.u.)$^{-3}$. Thus there is a definite contraction of this ion as it relaxes. This will be more evident from the results discussed in the next section.

C. Polarizability

With the method described in V-A, the total charge density as a function of the distance from a given center was used to find the screening parameter ζ for an equivalent Slater hydrogenic wave function. This was done for:

1) Free Li^+ and H^- ions described by the same Gaussian atomic orbitals as used for the crystal models.
2) Li^+ and H^- ions in LiH.
3) Li^+ and H^- ions and He in LiH:He, for two different values of relaxation of the nearest neighbor ions.

The values of ζ and the corresponding values of the polarizability, α, calculated from Eq. (20), are given in Table VI. Compared to the free-ion value of ζ for H^- of 0.64, found by using the Gaussian orbitals, the screening parameter for H^- in the crystalline state LiH has increased to 0.724, indicating a contraction of the ion in the crystal. As the H^- ion relaxes in the LiH:He state, ζ increases to

0.769 for $P_1 = 0.20$ and to 0.785 for $P_1 = 0.22$, indicating further contraction of the ion as it moves away from the lattice site.

It should be noted that Hurst's closed-shell function[15] gives an optimum value for the crystalline ζ of 0.7724 as compared to 0.6284 for the free ion. The free-ion values are not the same because, in the present calculation, the exponents for the two Gaussian orbitals used for H^- were not determined from the Slater free-ion value (0.6284), but were scaled from values for He as described in IV-B. In Hurst's calculations of the crystalline value, only one H^- ion was structured. It was surrounded by point ions to simulate the crystal field and the energy was minimized with respect to ζ, with perturbation terms in the Hamiltonian to take the effect of these point charges into account.

In the model used here, the six nearest neighbor Li^+ ions are structured, as well as six of the twelve second nearest H^- ions. In both calculations, the interionic distance was taken to be the experimental value. Comparison of the results found here with those of Hurst shows that there is less contraction of the H^- ion in the crystal field when there is structure on the ions surrounding it.

Hurst has noted that "the magnitude of the interaction between ... first nearest neighbor point charges and the electrons of H^- would be at a maximum if the central ion were a point charge. For this reason the central hy-

dride ion contracts until the interaction is offset by the increase in kinetic energy and electron-electron repulsion energies." The contraction of the central ion is less if there is structure on the surrounding ions presumably because of the additional kinetic energy and electron-electron repulsion energies due to this structure.

For the Li^+ ion, the value of δ for LiH is the same as that for LiH:He and is slightly larger than that for the free ion with two Gaussian orbitals. This is consistent with the contours shown in Figs. 9 and 12 and with Hurst's results which showed no contraction of the Li^+ ion in the crystal field. The screening parameter for the Li^+ ion found here is low compared to the usual free-ion value of 2.6875. The two values are not the same because the parameters used for the two Gaussian atomic orbitals were again not calculated from the single Slater value.

The polarizability of the H^- ion in the LiH crystal as found from the screening parameter is about 2.5 times the value of 1.93 $\mathring{A}^3$ found from the Lorentz-Lorentz relation given in Eq.(19). However, as determined from the screening parameters, the polarizability does decrease as the H^- ion is displaced from the lattice site. The 1.93 value corresponds more closely to the higher δ values used in the point-ion defect calculations.

The polarizability of the Li^+ ion is the same for the free ion and for the LiH and LiH:He states. It is about 1.4 times the Tessman, Kahn and Schockley[37] value of

0.029 $\AA^3$ determined from refractive data in crystals, but it is in reasonable agreement considering the small number of Gaussian orbitals that were used in computing what is a primary property. Sternheimer[50] has calculated the electronic polarizability of ions by considering the perturbation of the wave function by an external field. Using wave functions of Lowdin,[51] Sternheimer found a value of 0.03 $\AA^3$ for the Li^+ ion.

The screening parameter for the He atom is high compared to the free He parameter of 1.6875 found with the variation method. The nine Gaussian atomic orbitals were determined by Huzinaga[46] by a variational procedure. With the screening parameter found here the corresponding α value is lower than the 0.203 $\AA^3$ value used in the point-ion defect calculation. The latter value was determined from the single Slater value by Pauling.[24] The results obtained here show that there is some contraction of the He in LiH:He.

VI. Summary

The two-body interactions for the crystalline states LiH and LiH:He have been calculated by the Heitler-London method and used to determine repulsive interactions for point-ion models of these states. The model for LiH:He has been used to calculate formation and activation energies for the He defect.

A many-body model has also been constructed and an approximate solution of the Schrodinger equation has been found for the region in the vicinity of the defect. LCAO-MO-SCF calculations of formation and activation energies have been carried out with this model. The effect on the formation energy of the polarization of the ions near a face-centered interstitial defect has been studied by using orbitals with p-type symmetry, and results have been compared with classical calculations of the polarization energy in the point-ion defect model.

The total charge distribution in the defect region corresponding to the probability density found from the LCAO-MO-SCF calculations has been used to obtain charge density contours around the ion and defect sites in LiH and LiH:He. The radial variation in the charge density has been used to show contraction of the H^- ion in the crystal and to estimate the polarizabilities of the ions in the crystal field. A decrease in polarizability of the H^- ion with displacement from the lattice site has been demonstrated.

Table I

Born Mayer Parameters, Interionic Distance and Cohesive Energy

for First Nearest Neighbor Interactions only

	Screened Hydrogenic Functions					Hartree[a] - Fock	Hurst Crystal Open Shell[b]
	=0.6875	[illegible]	=0.82	[illegible]	[illegible]		
A in eV/molecule	1[illegible]5.78	[illegible]	2[illegible]3.[illegible]	2[illegible]7.38	2[illegible].2[illegible]	[illegible]	[illegible]
B in $Å^{-1}$	2.[illegible]	[illegible]	2.9635	3.2360	[illegible]	[illegible]	[illegible]
R_0 in Å	2.[illegible]	[illegible]	2.213	2.[illegible]	[illegible]	[illegible]	[illegible]
U in eV/ion pair	-8.34	-8.51	-9.63	-10.25	-10.[illegible]	[illegible]	[illegible]

a - Ref. 28

b - Ref. 15

TABLE II

Born Mayer Parameters for second nearest neighbor interactions. Crystal Parameters for first and second nearest neighbor interactions.

Screening Parameter of the H^- ion

	.6875	.7208	.82	.96	.[illegible]	Exp.
C in eV/molecule	13.4948	-7.7254	[illegible]	29.2[illegible]	[illegible]	
b in $Å^{-1}$	1.8301	2.3940	1.5297	1.8[illegible]	[illegible]	
R_o in Å	2.423	2.397	2.393	2.[illegible]	2.[illegible]	2.[illegible][a]
U in eV/ion pair	-8.69	-8.83	-9.22	-9.68	-[illegible]	-[illegible][b]
K in cm^2/dyne x 10^{-12}	3.70	3.43	2.74	2.22	[illegible]	[illegible][c]

a) See Ref 2

b) See Ref 29

c) This is the minimum experimental value reported. See Ref. 30. It also [illegible] discussion of theoretical minimum from other experimental values.

Table III

LiH Crystal Parameters from
other Investigators

Investigator	Cohesive Energy	Interionic Distance
Ellenbroek[a]	-9.07 eV/pair	7.71 A
Lundquist[b]	-8.70	7.84
Moriarty and Tibbetts[b]	-9.85	Not calculated
Hurst, Closed Shell[c]	-8.74	"
Hurst, Open Shell[c]	-10.3	"
Wilson and Johnson[d]		
Model I	-8.50	1.9%
Model II	-8.10	2.03%

* When interionic distance was not calculated, cohesive energy was calculated at the experimentally determined lattice distance. The latter is not necessarily the distance at which the minimum in the binding energy vs. interionic distance occurs.

a) See Ref. 13. The free ion values are used since the lattice parameter was obtained only for this case.

b) See Ref. 14.

c) See Ref. 15. Closed shell screened hydrogenic functions with δ 0.77 e.u. Open shell parameters are given elsewhere.

d) See Ref. 18.

Table IV

Gaussian Exponents for LCAO-MO-SCF

Calculations

H^-		0.0886	
		0.6840	
Li^+		1.30	nearest neighbor
		10.00	only
		2.6433	all other structures' ions
H.			
	n=2	[illegible]	
		0. [illegible] 321	
	n=9	0.129793	15.31660
		0.308364	55.41029
		0.725631	236.8036
		1.802569	1663.571
		4.951881	

TABLE V

Kinetic and Potential Energies in a.u.
at Minimum Separation Energy
for LiH and LiH:He

A. With s-type atomic orbitals

	Face Centered		Body Centered	
	T	V	T	V
LiH:He	84.716	-309.531	113.061	-359.091
LiH	81.788	-303.802	110.255	-353.468
T	2.928		2.806	
V		-5.729		-5.623
V/2		-2.865		-2.813

B. With s- and p-type atomic orbitals on H^-

	Face Centered	
	T	V
LiH:He	85.514	-307.565
LiH	79.877	-302.222
T	2.637	
V		-5.343
V/2		-2.672

Table VI

Orbital Exponents for He

Gaussian Exponent	Coefficients	
	Type 1s	Contracted 1s
0.129793	0.098809	0.098809
0.308367	0.315270	0.326081
0.725651	0.337783	0.333306
1.802969	0.244660	0.244568
4.951881	0.111758	0.113490
15.116660	0.038544	0.038527
55.410229	0.009939	0.009934
246.803656	0.001178	0.001176
1663.571	0.000093	0.000092

Table VII

Screening Parameters and Polarizabilities (in a_0^3) for LiH and Li_2H^+

	H^-		Li^+		H_2	
	1		2		1	
Free Ion or Atom	1.044	7.45	2.55	0.041	1.75	.21
LiH	.72*	2.89	2.41	0.040		
LiH_2^+						
P_1	.78*	3.54	2.41	0.040	1.77	.21
P_1	.755	3.5*	2.41	0.04	1.77	.21

* With same Gaussian orbitals as used in crystal calculation

Fig. 1 $Li^+ - H^-$ repulsive interactions for various H^- wave functions.

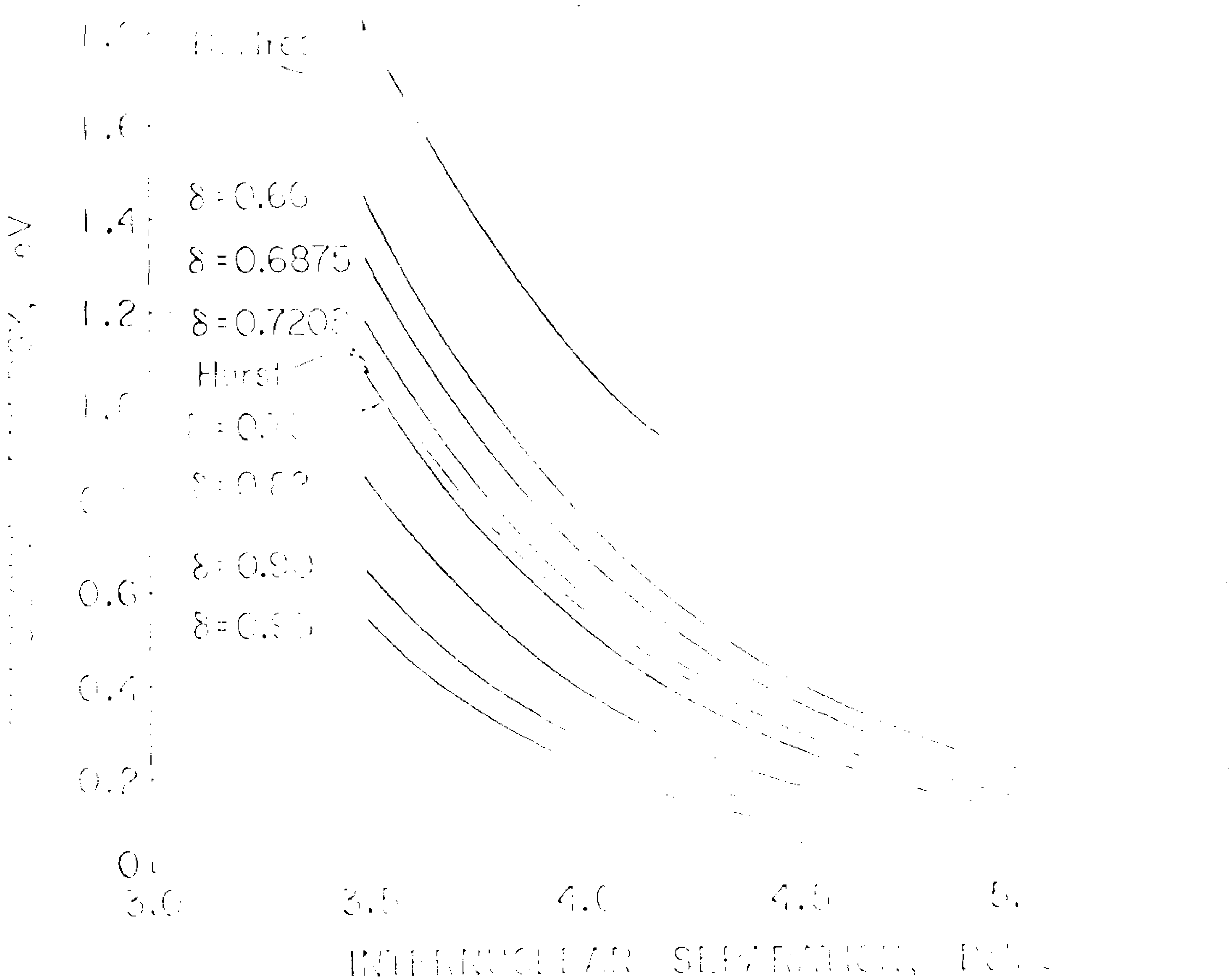
δ = 0.66
δ = 0.6875
Hurst
1.4
1.2
0.6
0.4
0
3.0
4.0

Fig. 2 H^- - H^- repulsive interactions for various H^- wave functions.

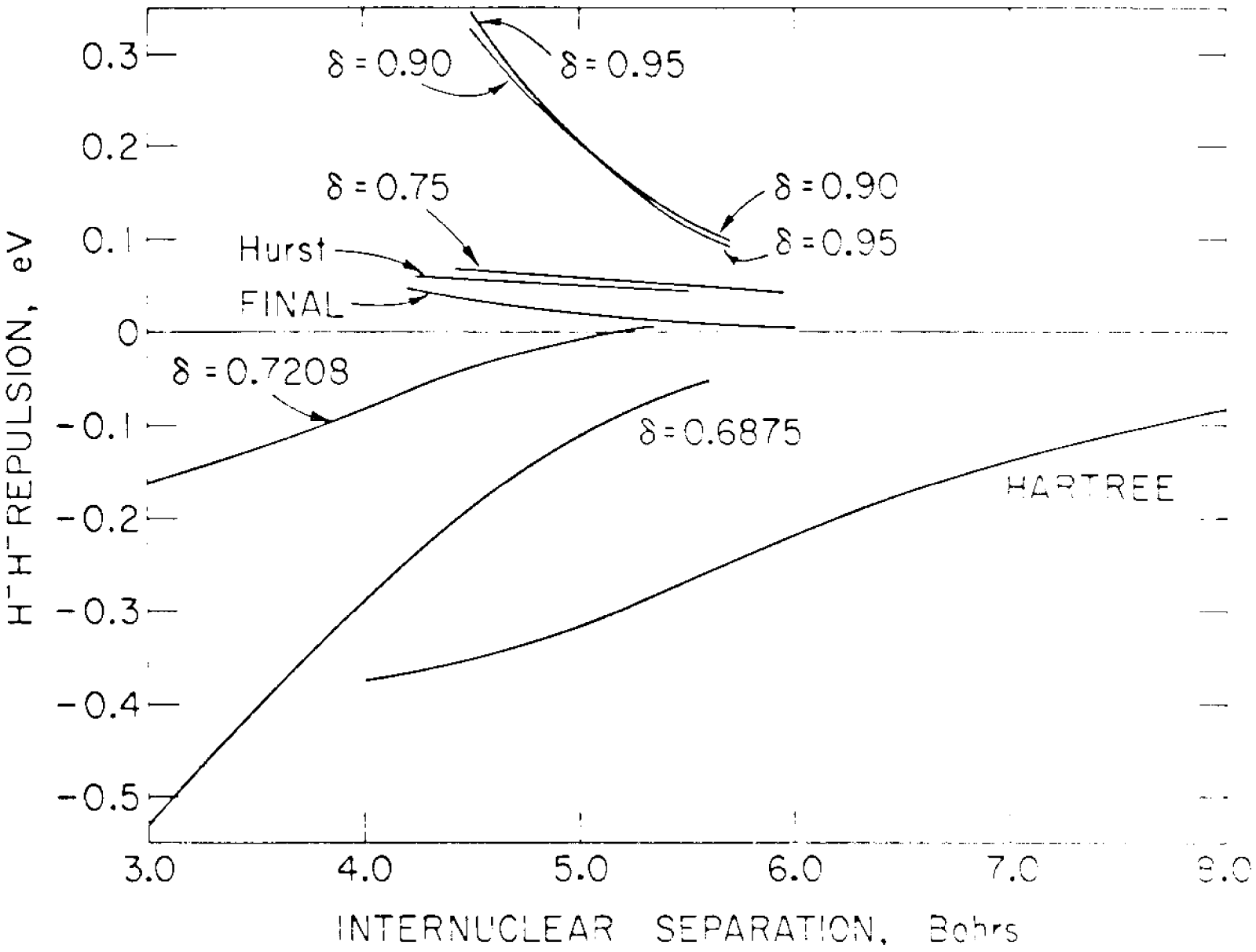
δ = 0.90
δ = 0.95
δ = 0.75
δ = 0.90
δ = 0.95
Hurst
FINAL
δ = 0.7208
δ = 0.6875
HARTREE
0.3
0.2
0.1
0
-0.1
-0.2
-0.3
-0.4
-0.5
3.0
4.0
5.0
6.0
7.0
8.0
H⁻H⁻ REPULSION, eV
INTERNUCLEAR SEPARATION, Bohrs

Fig. 3 Positions of structured ions for body-centered defect calculations in LiH:He.

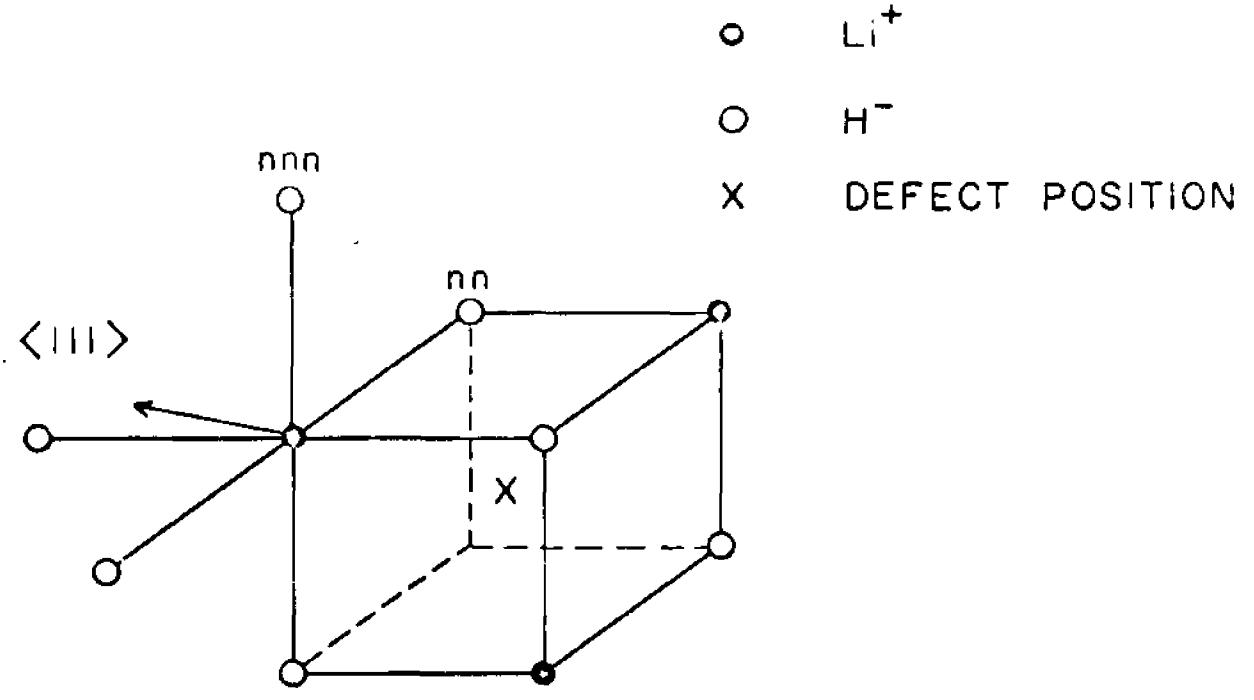

BODY-CENTERED LiH:He

Fig. 4 Positions of structured ions for face-centered defect calculations in LiH:He.

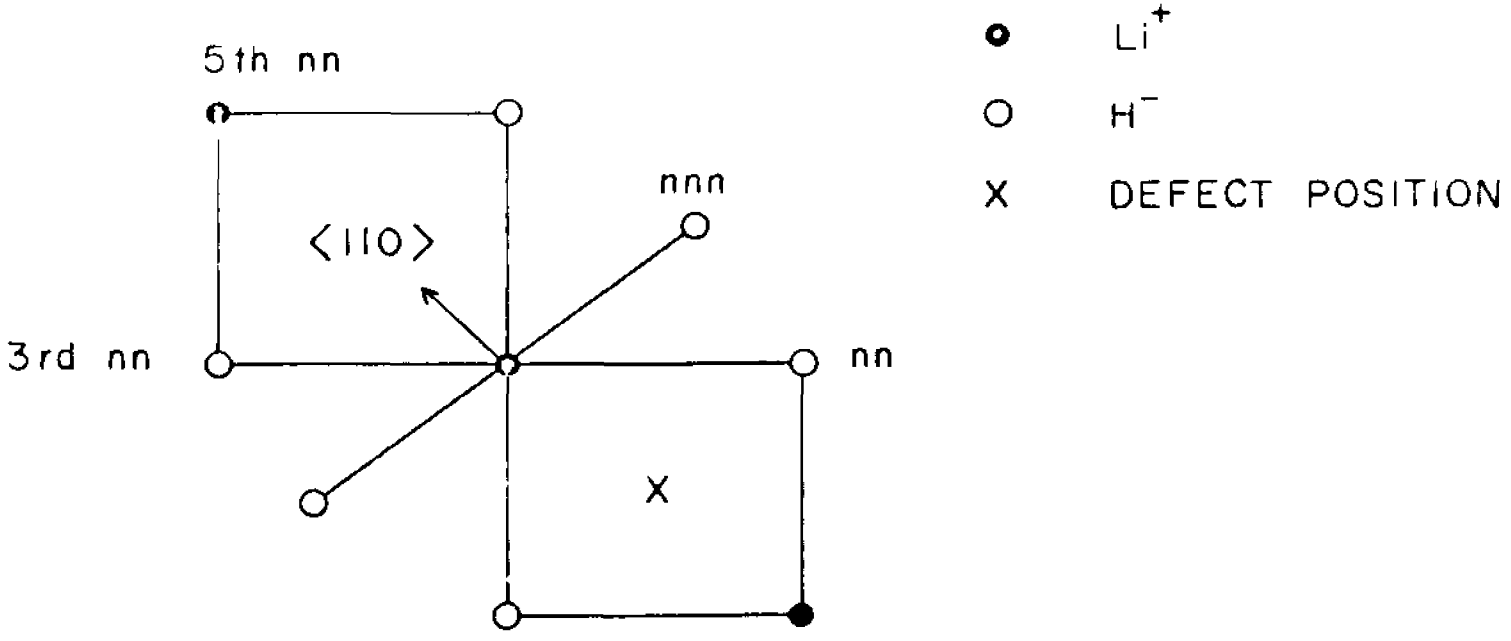

FACE-CENTERED LiH:He

Fig. 5 LCAO-MO-SCF formation energy for body-centered He defect in LiH versus relaxation of nearest-neighbor H^- ion, with s-type atomic orbitals.

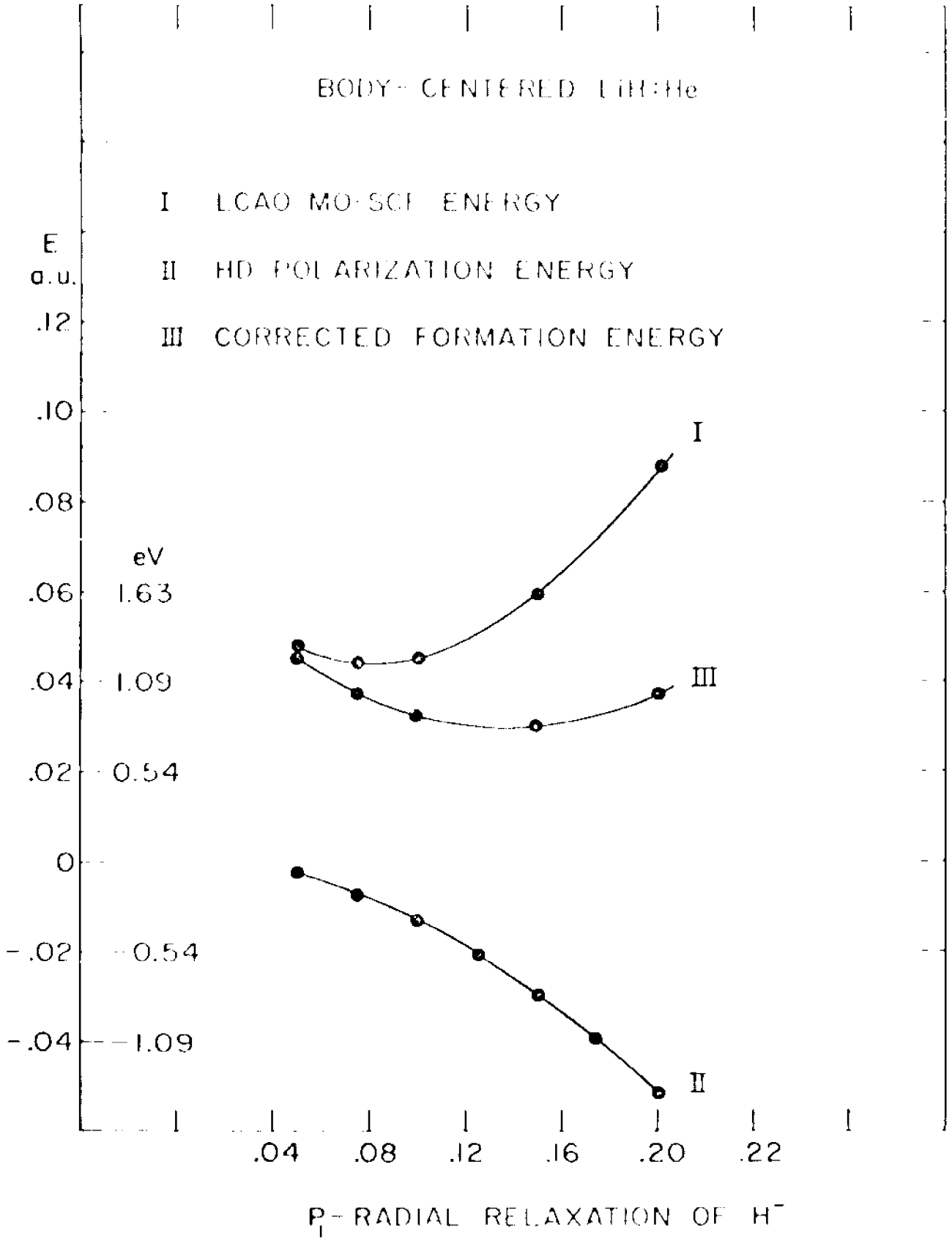
BODY-CENTERED LiH:He
I LCAO MO-SCF ENERGY
II HD POLARIZATION ENERGY
III CORRECTED FORMATION ENERGY
E
a.u.
.12
.10
.08
.06
.04
.02
0
-.02
-.04
eV
1.63
1.09
0.54
0.54
1.09
I
III
II
.04
.08
.12
.16
.20
.22
P_1 - RADIAL RELAXATION OF H^-

Fig. 6 LCAO-MO-SCF formation energy for face-centered He defect in LiH versus relaxation of nearest-neighbor H^- ion, with s-type atomic orbitals.

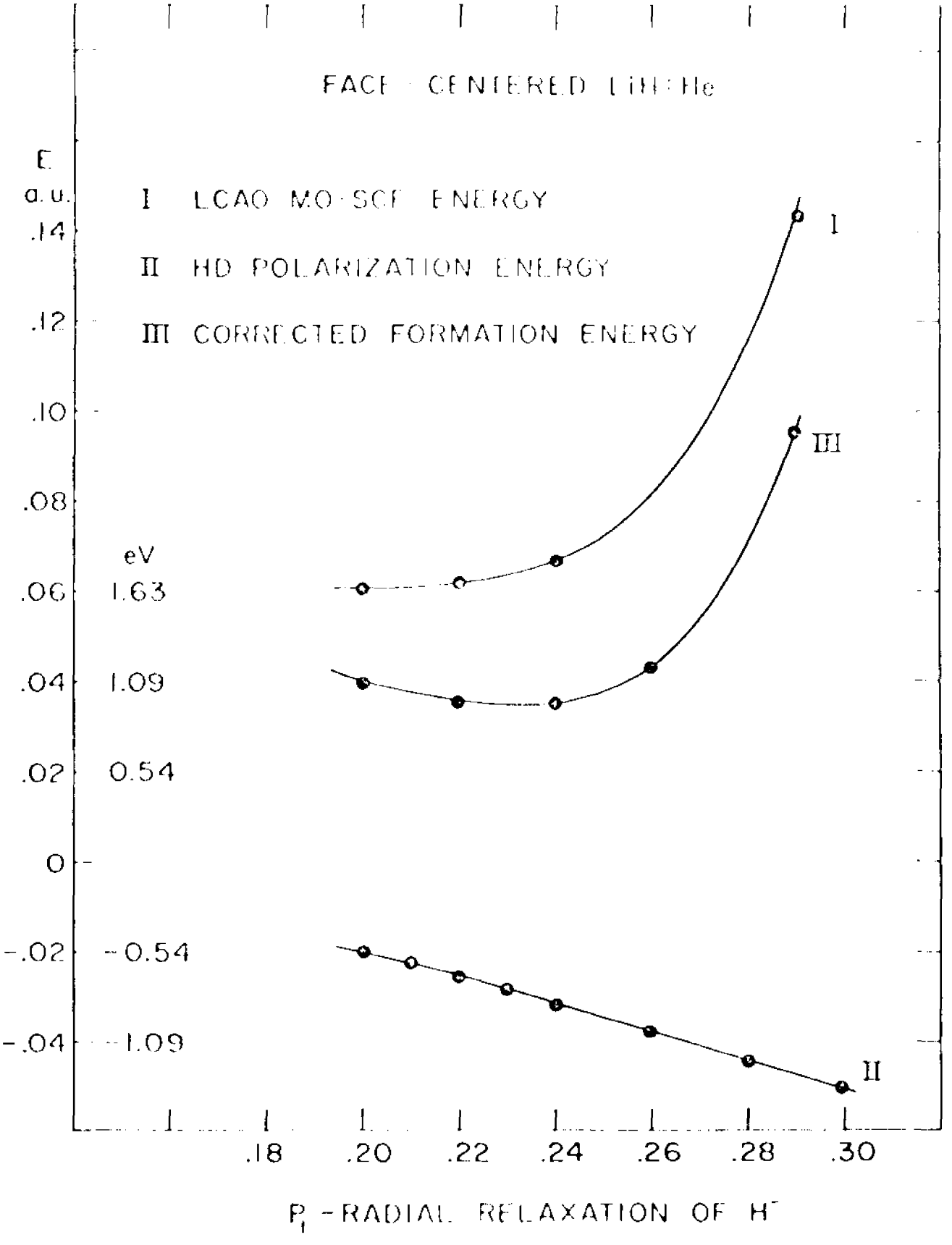
FACE CENTERED LiH:He
E
a.u.
I LCAO MO-SCF ENERGY
II HD POLARIZATION ENERGY
III CORRECTED FORMATION ENERGY
.14
.12
.10
.08
.06
.04
.02
0
-.02
-.04
eV
1.63
1.09
0.54
-0.54
-1.09
I
III
II
.18
.20
.22
.24
.26
.28
.30
P1 - RADIAL RELAXATION OF H⁻

Fig. 7 LCAO-MO-SCF energy for face-centered He defect in LiH versus relaxation of nearest-neighbor H^- ion, with s- and p-type atomic orbitals.

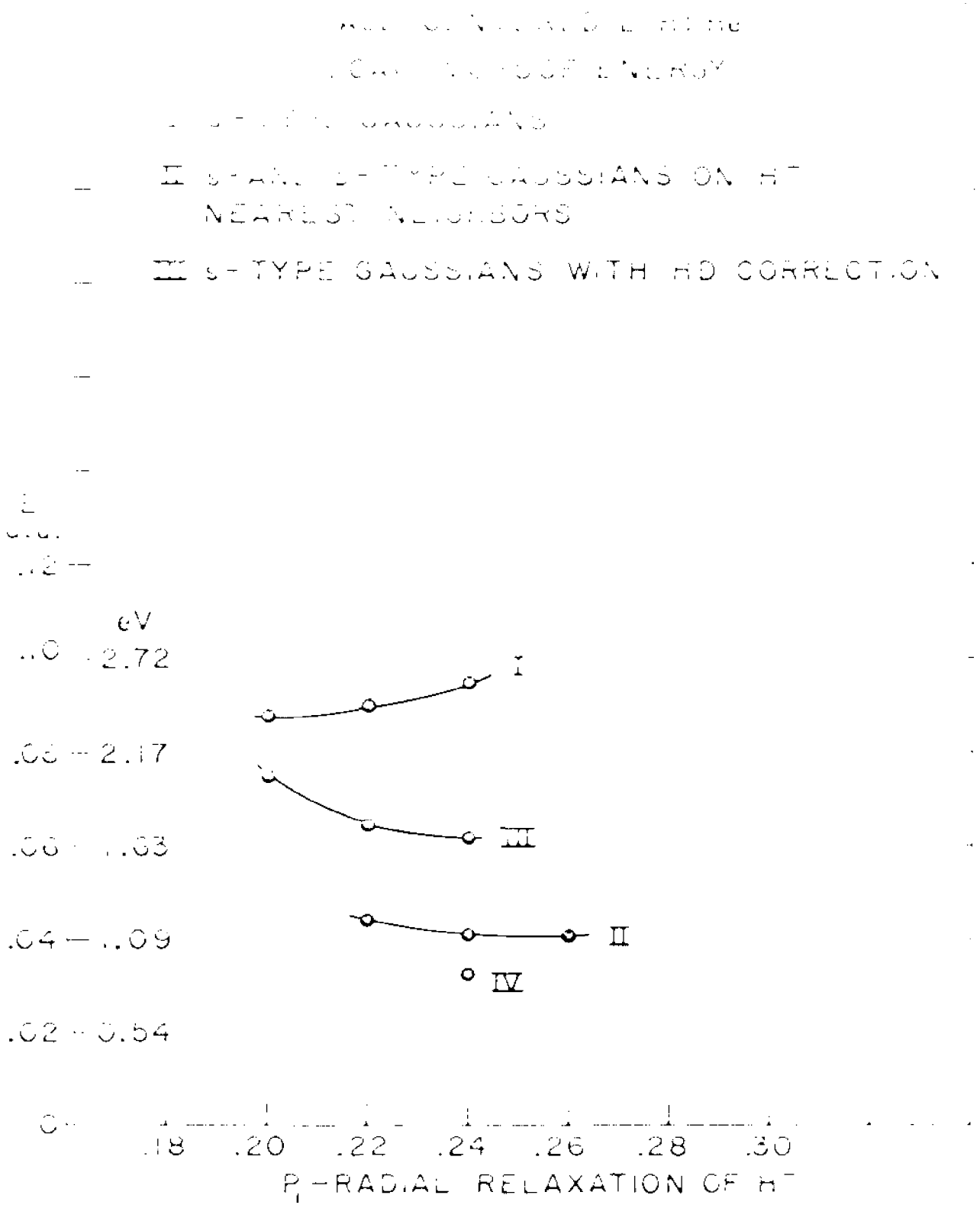
II S-TYPE GAUSSIANS ON H⁻
NEAREST NEIGHBORS
III S-TYPE GAUSSIANS WITH HD CORRECTION
eV
.0 — 2.72
.08 — 2.17
.06 — .03
.04 — .09
.02 — 0.54
I
III
II
IV
.18
.20
.22
.24
.26
.28
.30
P₁ — RADIAL RELAXATION OF H⁻

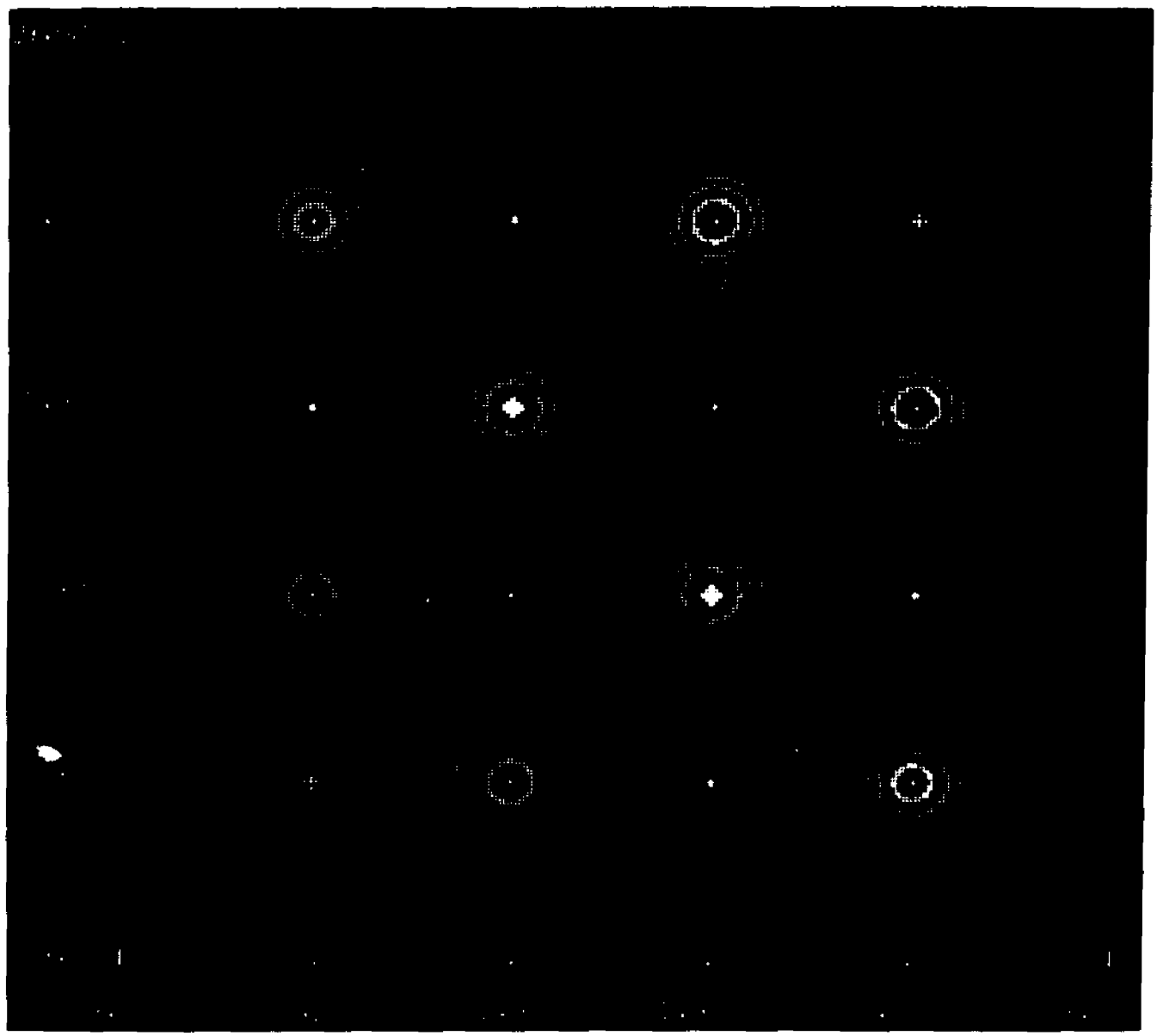

Fig. 8 Charge density contours in the vicinity of H^- ions in LiH. Maximum density is 0.0917 $(a.u.)^{-3}$

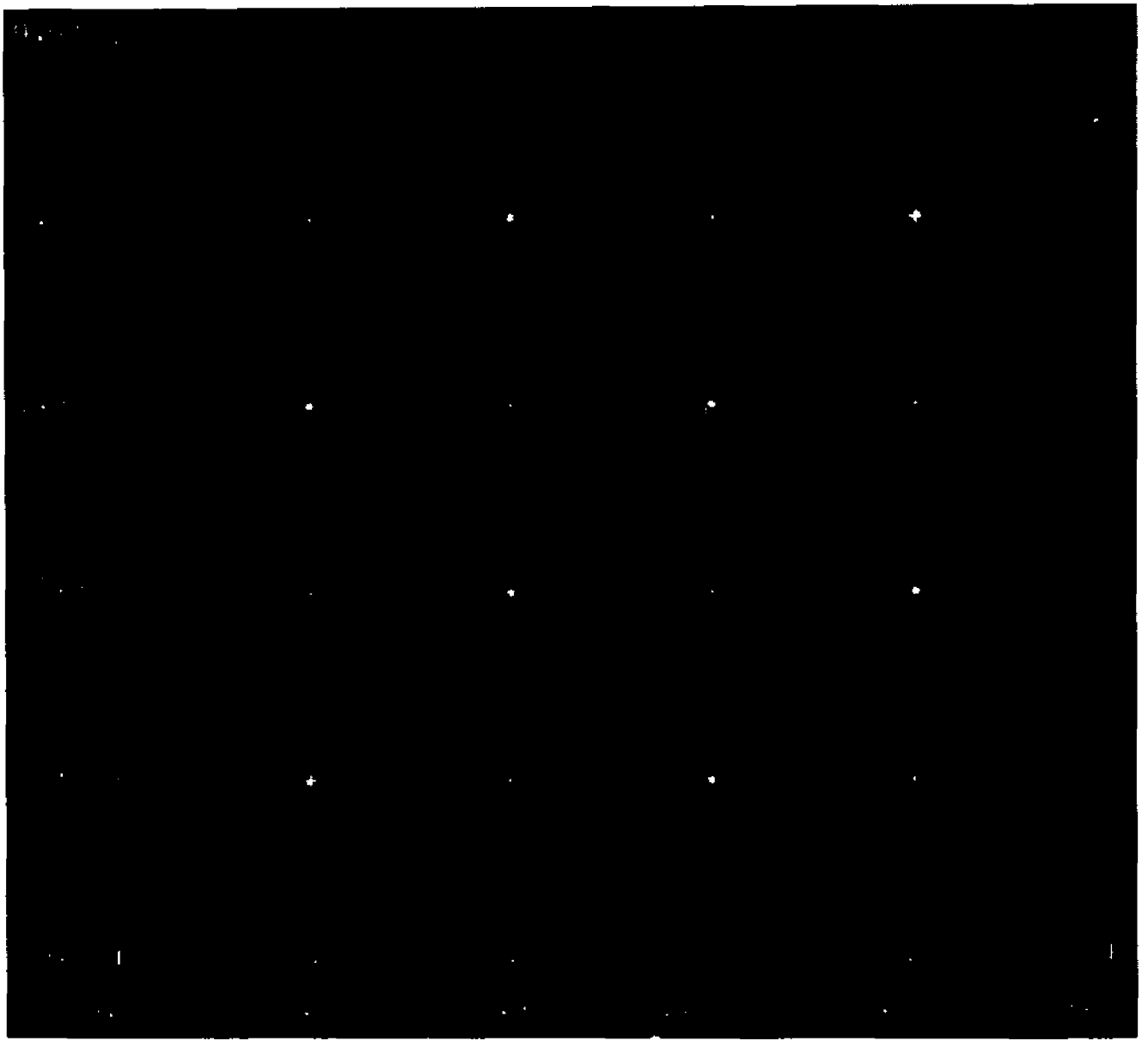

Fig. 9 Charge density contours in the vicinity of Li^+ ions in LiH. Maximum density is 3.4526 $(a.u.)^{-3}$

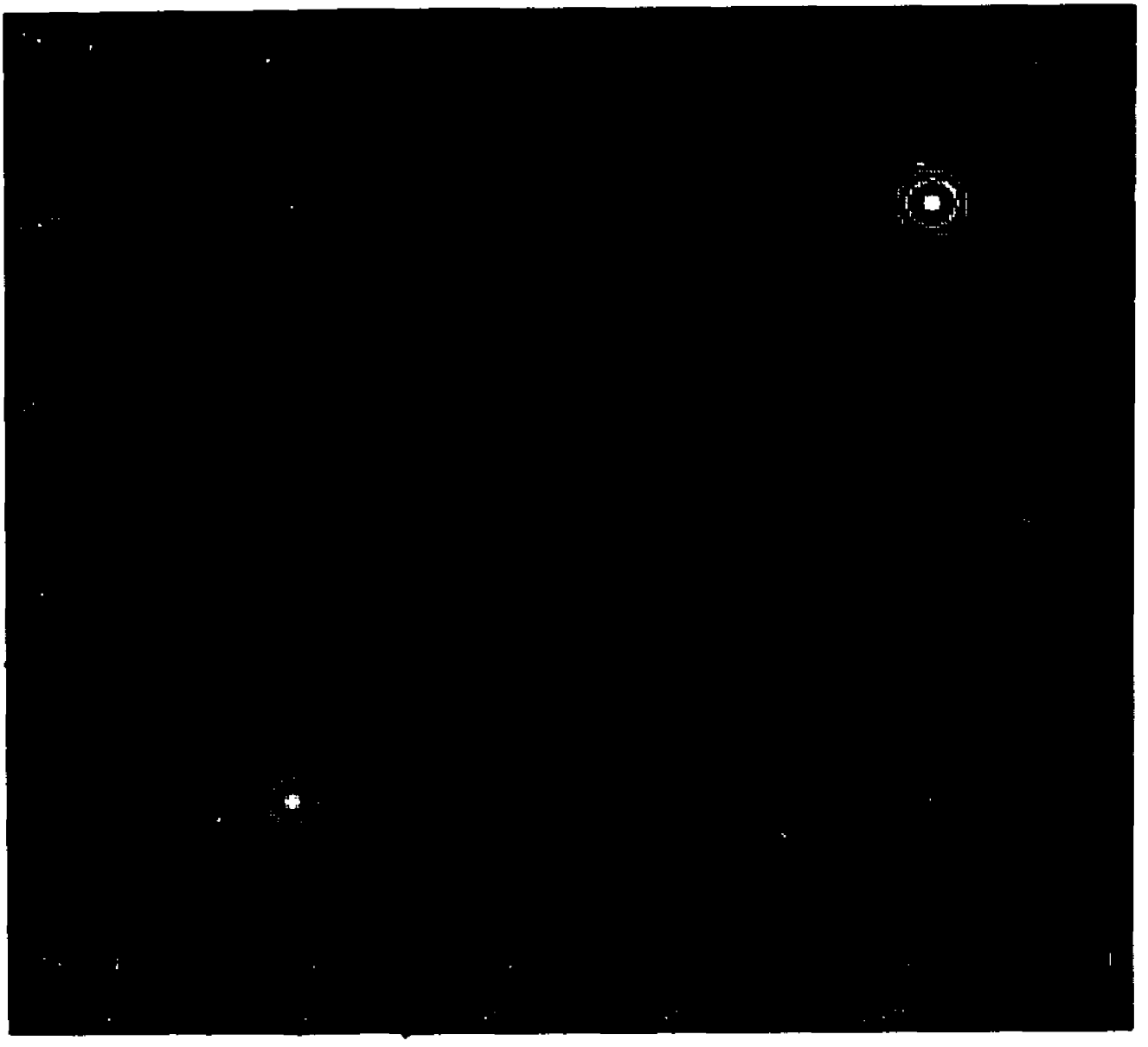

Fig. 10 Charge density contours for molecular orbital with lowest orbital energy in LiH. Maximum density is 1.7261 $(a.u.)^{-3}$ Orbital energy is -2.3870 a.u.

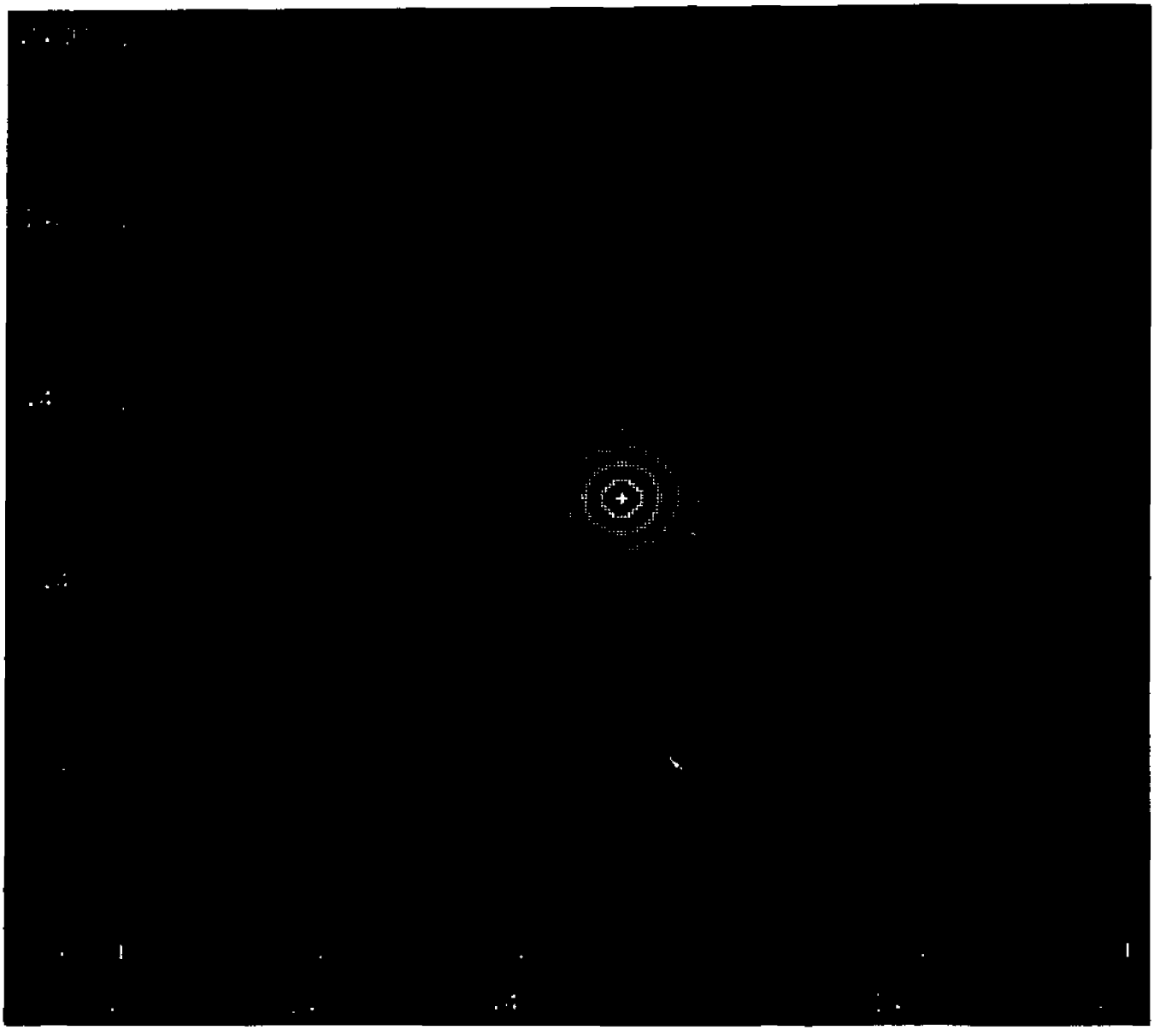

Fig. 11 Charge density contours for He defect in LiH:He. Maximum density is 1.6265 $(a.u.)^{-3}$ Orbital energy is -1.1095 a.u.

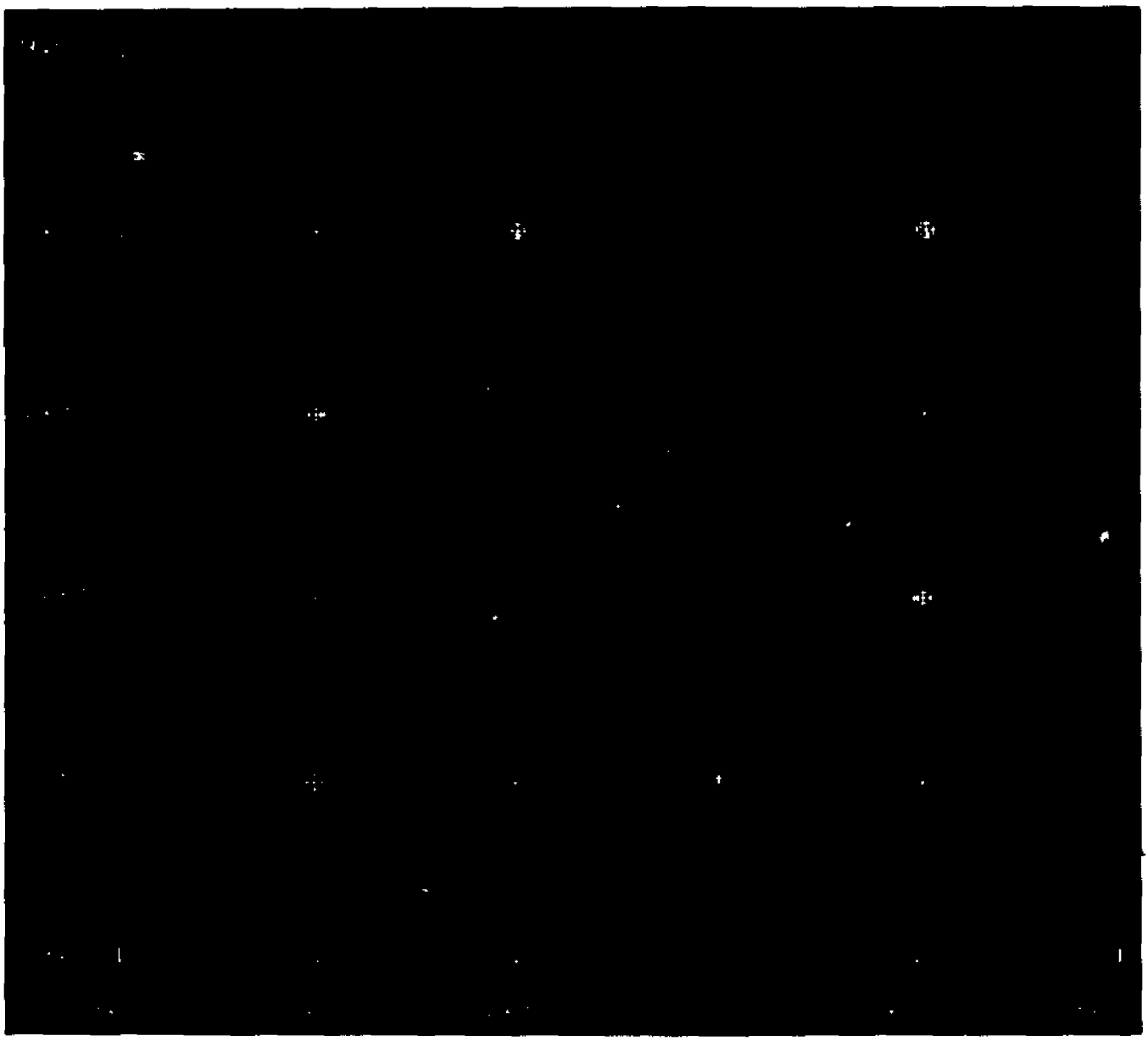

Fig. 12 Charge density contours in the vicinity of Li^+ ions in LiH:He. Maximum density is 3.1353 $(a.u.)^{-3}$

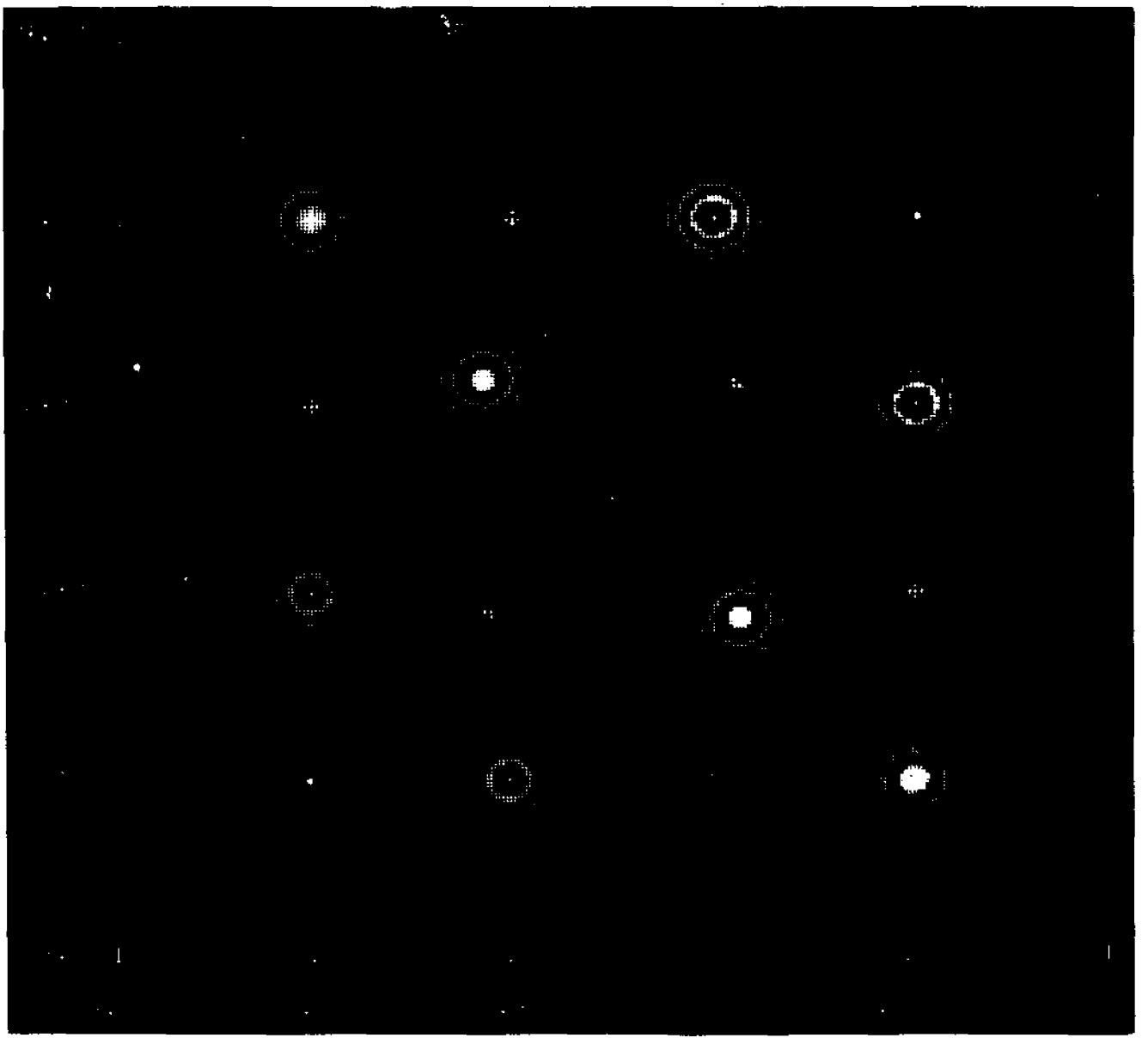

Fig. 13 Charge density contours in the vicinity of H^- ions in LiH:He. Maximum density is 0.0967 $(a.u.)^{-3}$

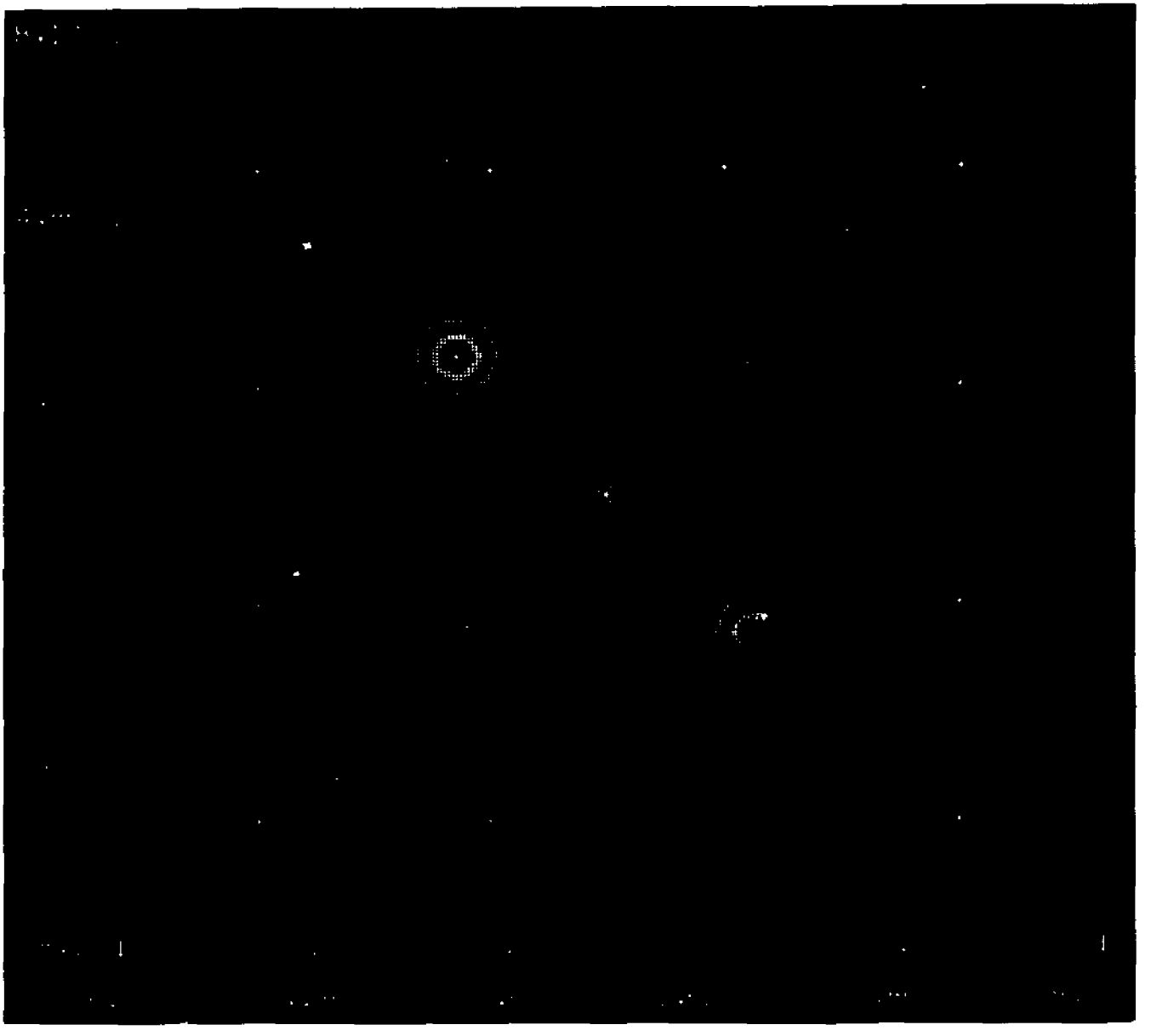

Fig. 14 Charge density contours for molecular orbital with highest orbital energy in LiH;He. Maximum density is 0.0513 $(a.u.)^{-3}$ Orbital energy is -0.3728 a.u.

Appendix A

The open configuration energy for a heteronuclear four-electron system can be evaluated following the work of Rosen[52] for evaluating the repulsive potential of normal He atoms. The unsymmetrized wave function for a four-electron system with spin included can be written as

$$\zeta = a(1)\alpha(1)b(2)\beta(2)c(3)\alpha(3)d(4)\beta(4) \qquad \text{(A-1)}$$

where a and b are 1s hydrogenic atomic orbitals for center one and are of the form

$$a = (\delta_1^3/\pi)^{\frac{1}{2}}\, e^{-\delta_1 r}$$
$$b = (\delta_2^3/\pi)^{\frac{1}{2}}\, e^{-\delta_2 r} \qquad \text{(A-2)}$$

where δ_1 and δ_2 are open-shell parameters. For a(1) and b(2), the coordinates refer to electron 1 and electron 2, respectively. Functions c(3) and d(4) are similar functions for center two with open-shell parameters δ_3 and δ_4 and with coordinates referring to electrons 3 and 4. For the helium problem, $\delta_1 = \delta_3$ and $\delta_2 = \delta_4$.

Hurst[15] has used an open configuration antisymmetrized two-electron function for a single ion in LiH, either Li^+ or H^-, in a crystalline field. This function is written as

$$\zeta(1,2) = [a(1)b(2) + a(2)b(1)] \times [\alpha(1)\beta(2) - \alpha(2)\beta(1)] \qquad \text{(A-3)}$$

For the two centers considered here, the two-electron functions may be written as

$$\zeta_k(1,2) = |a\alpha b\beta| + |b\alpha a\beta|$$
$$\zeta_l(3,4) = |c\alpha d\beta| + |d\alpha c\beta| \qquad \text{(A-4)}$$

The four-electron function will then be of the form

$$\psi_p(1234) = \zeta_k(1,2)\zeta_l(3,4) \qquad \text{(A-5)}$$

The total antisymmetrized wave function can be constructed by permuting the four electrons on the two centers. Thus

$$\psi(1234) = \frac{1}{\sqrt{4!}} \sum (-1)^p \psi_p(1234) \qquad \text{(A-6)}$$

which gives

$$\psi(1234) = \frac{4}{\sqrt{4!}} \{ |\alpha_k(12)\alpha_l(34) + \alpha_k(34)\alpha_l(12)| + |\alpha_k(23)\alpha_l(14) + \alpha_k(14)\alpha_l(23)| - |\alpha_k(13)\alpha_l(24) + \alpha_k(24)\alpha_l(13)| \} \qquad \text{(A-7)}$$

This can be shown to be equivalent to

$$\psi_A = \psi_1 - \psi_2 - \psi_3 + \psi_4 \qquad \text{(A-8)}$$

where

$$\psi_1 = |a\alpha b\beta c\alpha d\beta| \qquad \psi_3 = |a\alpha b\alpha c\alpha d\alpha|$$
$$\psi_2 = |a\beta b\alpha c\alpha d\alpha| \qquad \psi_4 = |a\beta b\alpha c\beta d\alpha|$$

The total energy is given by

$$E = \frac{H_{AA}}{\Delta_{AA}} = \frac{\int \psi_A^* H_T \psi_A d\tau}{\int \psi_A \psi_A d\tau} \qquad \text{(A-9)}$$

where

$$H_{AA} = 4Q - 2\sum|ij| - 2\sum|ijk| + 4\sum|(ij)(kl)| - 2\sum|ijkl| \qquad \text{(A-10)}$$

The integral Q is given by

$$Q = \int a(1)b(2)c(3)d(4)H_1 a(1)b(2)c(3)d(4)\, d\tau \qquad \text{(A-11)}$$

and the integrals corresponding to the brackets are obtained by cyclically permuting the electrons in the integral Q as follows

$$|ij| = a(i)b(j)c(k)d(l)H_1 a(j)b(i)c(k)d(l)\, d\tau$$

$$|ijk| = a(i)b(j)c(k)d(l)H_1 a(j)b(k)c(i)d(l)\, d\tau$$

$$|(ij)(kl)| = a(i)b(j)c(k)d(l)H_1 a(j)b(i)c(l)d(k)\, d\tau$$

$$|ijkl| = a(i)b(j)c(k)d(l)H_1 a(j)b(k)c(l)d(i)\, d\tau$$

The remaining terms in Eq. (A-10) are

$$\sum|ij| = |13| + |14| + |23| + |24| - 2|12| - 2|34| \qquad \text{(A-12)}$$

$$\sum|ijk| = |134| + |243| + |123| + |142| + |124| + |132| + |234| + |143| \qquad \text{(A-13)}$$

$$\sum|(ij)(kl)| = |(13)(24)| + |(14)(23)| + |(12)(34)| \qquad \text{(A-14)}$$

$$\sum|ijkl| = |1234| + |1432| + |1243| + |1342| - 2|1423| - 2|1324| \qquad \text{(A-15)}$$

The expression for Δ_{AA} can be obtained by replacing H_1 by unity in all of the integrals in H_{AA}. The Hamiltonian for the four-electron case is given by

$$H_i = -\tfrac{1}{2}\nabla_i^2 - \frac{Z_k}{r_i} - \frac{Z_l}{r_i'} + \sum_{j>i}\frac{1}{r_{ij}} + \frac{Z_k Z_l}{R} \qquad \text{(A-16)}$$

where Z_k and Z_l are the nuclear charges, R is the internuclear separation and the summation runs over the four electrons. When this Hamiltonian is substituted into Eq. (A-9), various one- and two-center integrals result. The following notation will be used

$$a = s_1 \qquad c = h_1$$
$$b = s_2 \qquad d = h_2$$

where s refers to Li^+ and h refers to H^-. Table A-1 lists the integral types with examples of each.

The two-center one-electron integrals are single charge distributions shared by two centers (overlap), charge distributions on a single center interacting with a point charge on the second center (nuclear attraction), or a charge distribution shared by two centers interacting with a point charge at one of these centers (split nuclear attraction). The two-center two-electron integrals correspond to the interaction between two charge distributions. For Coulomb integrals, both charge distributions are single-centered. In exchange integrals, both charge distributions are shared by the two centers.

If the one-electron operators in the Hamiltonian are written as

$$h_i = -\frac{\nabla_i^2}{2} - \frac{Z_k}{r_k} - \frac{Z_l}{r_l},$$

and the two-electron integrals are written with $1/r_{12}$

Table A-1

Integral Type	Example
1. One-center	
a) one-electron	
electron charge	$(s_1 \mid s_1)$
nuclear attraction	$(s_1 \mid \frac{1}{r} \mid s_1)$
b) two-electron	
Coulomb	$(s_1 s_2 \mid \frac{1}{r} \mid s_1 s_2)$
2. Two-center	
a) one-electron	
overlap	$(h_1 \mid s_1)$
nuclear attraction	$(s_1 \mid \frac{1}{r} \mid s_1)$
split nuclear	$(h_1 \mid \frac{1}{r} \mid s_1)$
b) two-electron	
Coulomb	$(h_1 h_2 \mid \frac{1}{r} \mid s_1 s_2)$
hybrid	$(h_1 h_1 \mid \frac{1}{r} \mid h_1 s_1)$
exchange	$(h_1 s_1 \mid \frac{1}{r} \mid h_1 s_1)$

understood, the quantities in H_{AA} become

$$\begin{aligned} Q = &(s_1|H|s_1) + (s_2|H|s_2) + (h_1|H|h_1) \\ &+ (h_2|H|h_2) + (s_1s_2|s_1s_2) \\ &+ (s_1h_1|s_1h_1) + (s_1h_2|s_1h_2) \\ &+ (s_2h_1|s_2h_1) + (s_2h_2|s_2h_2) + (h_1h_2|h_1h_2) \end{aligned} \tag{A-17}$$

$$\begin{aligned} (ij) = &(s_1|H|s_1)(h_1|s_2)^2 + (h_2|s_2)^2 - 2(h_1|h_2)^2 \\ &+ (s_2|H|s_2)(h_1|s_1)^2 + (h_2|s_1)^2 - 2(h_1|h_2)^2 \\ &+ (h_1|H|h_1)(h_2|s_1)^2 + (h_2|s_2)^2 - 2(s_1|s_2)^2 \\ &+ (h_2|H|h_2)(h_1|s_1)^2 + (h_1|s_2)^2 - 2(s_1|s_2)^2 \\ &- 4[(s_1|s_2)(s_1|H|s_2) + (h_1|h_2)(h_1|H|h_2)] \\ &+ 2[(h_1|s_1)(h_1|H|s_1) + (h_1|s_2)(h_1|H|s_2) \\ &\quad + (h_2|s_2)(h_2|H|s_2) + (h_2|s_1)(h_2|H|s_1)] \\ &+ (h_2|s_2)^2(h_1h_1|s_1s_1) + (h_1|s_2)^2(h_2h_2|s_1s_1) \\ &+ (h_2|s_1)^2(h_1h_1|s_2s_2) + (h_1|s_1)^2(h_2h_2|s_2s_2) \\ &- 2(h_1|h_2)^2(s_1s_1|s_2s_2) - 2(s_1|s_2)^2(h_1h_1|h_2h_2) \\ &- 2[(h_1|s_2)[(h_1s_2|s_1s_1) + (h_1s_2|h_2h_2)] \\ &\quad + (h_2|s_2)[(h_2s_2|s_1s_1) + (h_2s_2|h_1h_1)] \\ &\quad + (h_1|s_1)[(h_1s_1|s_2s_2) + (h_1s_1|h_2h_2)] \\ &\quad + (h_2|s_1)[(h_2s_1|s_2s_2) + (h_2s_1|h_1h_1)] \\ &\quad + 2(s_1|s_2)[(h_1h_1|s_1s_2) + (h_2h_2|s_1s_2)] \\ &\quad + 2(h_1|h_2)[(h_1h_2|s_1s_1) + (h_1h_2|s_2s_2)]] \\ &+ (h_1s_1|h_1s_1) + (h_2s_1|h_2s_1) + (h_1s_2|h_1s_2) \\ &+ (h_2s_2|h_2s_2) - 2(s_1s_2|s_2s_1) - 2(h_1h_2|h_1h_2) \end{aligned} \tag{A-18}$$

$$
\begin{aligned}
\tfrac{1}{2}(1jk) = {} & (s_1|H|s_1)(h_1|h_2)(h_1|s_2)(h_2|s_2) \\
& + (s_1|H|s_2)\left[(h_1|s_1)(h_1|s_2) + (h_2|s_1)(h_2|s_2)\right] \\
& + (s_2|H|s_2)(h_1|s_1)(h_1|h_2)(h_2|s_1) \\
& + (h_1|H|h_1)(h_2|s_1)(h_2|s_2)(s_1|s_2) \\
& + (h_1|H|h_2)\left[(h_1|s_1)(h_2|s_2) + (h_1|s_1)(h_2|s_1)\right] \\
& + (h_2|H|h_2)(h_1|s_1)(h_1|s_2)(s_1|s_2) \\
& + (h_1|H|s_1)\left[(h_1|h_2)(h_2|s_1) + (h_1|s_2)(s_1|s_2)\right] \\
& + (h_1|H|s_2)\left[(h_1|h_2)(h_2|s_2) + (h_1|s_1)(s_1|s_2)\right] \\
& + (h_2|H|s_2)\left[(h_1|h_2)(h_1|s_2) + (h_2|s_1)(s_1|s_2)\right] \\
& + (h_2|H|s_1)\left[(h_1|h_2)(h_1|s_1) + (h_2|s_2)(s_1|s_2)\right] \\
& + (s_1|s_2)\left[(h_2|s_2)(h_2s_1|h_1h_1) + (h_2|s_1)(h_2s_2|h_1h_1)\right. \\
& \qquad + (h_1|s_2)(h_1s_1|h_2h_2) + (h_1|s_1)(h_1s_2|h_2h_2) \\
& \qquad \left. + (h_1s_1|s_2h_1) + (h_2s_2|s_1h_2)\right] \\
& + (h_1|s_1)\left[(h_2|s_1)(h_1h_2|s_2s_2) + (h_1|s_2)(h_2h_2|s_1s_2)\right. \\
& \qquad \left. + (h_1|h_2)(h_2s_1|s_1s_2) + (h_2s_1|h_1h_2)\right] \\
& + (h_2|s_1)\left[(h_2|s_2)(h_1h_1|s_1s_2) + (h_1|h_2)(h_1s_1|s_2s_2)\right. \\
& \qquad \left. + (h_2s_2|s_1s_2) + (h_1s_1|h_2h_1)\right] \\
& + (h_1|s_2)\left[(h_2|s_2)(h_1h_2|s_1s_1) + (h_1|h_2)(h_2s_2|s_1s_1)\right. \\
& \qquad \left. + (h_1s_1|s_1s_2) + (h_1s_2|s_1s_2) + (h_2s_2|h_1h_2)\right] \\
& + (h_2|s_2)\left[(h_1|h_2)(h_1s_2|s_1s_1) + (h_2s_1|s_1s_2)\right. \\
& \qquad \left. + (h_1s_2|h_2h_1)\right] \\
& + (h_1|h_2)\left[(h_1s_1|s_1h_2) + (h_1s_2|s_2h_2)\right]
\end{aligned}
\tag{A-19}
$$

$$
\begin{aligned}
(1j)(kl) = {} & 2(s_1|H|s_2)(s_1|s_2)(h_1|h_2)^2 \\
& + 2(h_1|H|h_2)(s_1|s_2)^2(h_1|h_2) \\
& + 2(h_1|H|s_1)(h_2|s_2)^2(h_1|s_1) \\
& + 2(h_1|H|s_2)(h_2|s_1)^2(h_1|s_2) \\
& + 2(h_2|H|s_2)(h_1|s_1)^2(h_2|s_2) \\
& + 2(h_2|H|s_1)(h_1|s_2)^2(h_2|s_1) \\
& + (h_1|h_2)^2(s_1s_2|s_2s_1) + (s_1|s_2)^2(h_1h_2|h_2h_1) \\
& + (h_2|s_2)^2(h_1s_1|s_1h_2) + (h_1|s_2)^2(h_2s_1|s_1h_2) \\
& + (h_2|s_1)^2(h_1s_2|s_2h_1) + (h_1|s_1)^2(h_2s_2|s_2h_2) \\
& + 4(h_1|h_2)(s_1|s_2)(h_1h_2|s_1s_2) \\
& + 4(h_1|s_1)(h_2|s_2)(h_1s_1|h_2s_2) \\
& + 4(h_1|s_2)(h_2|s_1)(h_2s_1|h_1s_2)
\end{aligned}
\tag{A-20}
$$

$$
\begin{aligned}
+ (1jkl) = {} & \big[(s_1|H|s_2)(h_1|h_2) + (h_1|H|h_2)(s_1|s_2)\big] \\
& \quad \times \big[(h_2|s_1)(h_1|s_2) + (h_2|s_1)(h_1|s_1)\big] \\
& + \big[(h_1|H|s_1)(h_2|s_2) + (h_2|H|s_2)(h_1|s_1)\big] \\
& \quad \times \big[(h_1|h_2)(s_1|s_2) - 2(h_1|s_2)(h_2|s_1)\big] \\
& + \big[(h_1|H|s_2)(h_2|s_1) + (h_2|H|s_1)(h_1|s_2)\big] \\
& \quad \times \big[(h_1|h_2)(s_1|s_2) - 2(h_1|s_1)(h_2|s_2)\big] \\
& + \big[(h_1|s_2)(h_2|s_1) + (h_1|s_1)(h_2|s_2)\big](h_1h_2|s_1s_2) \\
& + (h_1|h_2)\big[(h_2|s_2)(s_1s_2|h_1s_1) + (h_2|s_1)(s_1s_2|s_2h_1) \\
& \quad + (h_1|s_2)(s_1s_2|h_2s_1) + (h_1|s_1)(s_1s_2|s_2h_2)\big] \\
& + (s_1|s_2)\big[(h_2|s_2)(h_1h_2|s_1h_1) + (h_2|s_1)(h_1h_2|s_2h_1) \\
& \quad + (h_1|s_2)(h_1h_2|h_2s_1) + (h_1|s_1)(h_1h_2|h_2s_2)\big] \\
& - 2(h_2|s_2)\big[(h_1|s_2)(h_1s_1|s_1h_2) + (h_2|s_1)(h_1s_1|s_2h_1)\big] \\
& - 2(h_1|s_1)\big[(h_1|s_2)(h_2s_2|s_1h_2) + (h_2|s_1)(h_2s_2|s_2h_1)\big] \\
& + \big[(h_1|h_2)(s_1|s_2) - 2(h_1|s_1)(h_2|s_2)\big](h_1s_2|s_1h_2) \\
& + \big[(h_1|h_2)(s_1|s_2) - 2(h_1|s_2)(h_2|s_1)\big](h_1s_1|s_2h_2)
\end{aligned}
\tag{A-21}
$$

The quantity Λ_{AA} is given by

$$\begin{aligned}\Lambda_{AA} = 4 &- 2\left\{(h_1|s_1)^2 + (h_2|s_1)^2 + (h_1|s_2)^2 + (h_2|s_2)^2\right\} \\ &+ 4\left\{(s_1|s_2)^2 + (h_1|h_2)^2\right\} \\ &- 4\left\{(h_1|h_2)\left[(h_1|s_2)(h_2|s_2) + (h_1|s_1)(h_2|s_1)\right]\right. \\ &\quad + (s_1|s_2)\left[(h_1|s_2)(h_1|s_1) + (h_2|s_1)(h_2|s_2)\right] \\ &+ 4\left[(h_1|s_1)^2(h_2|s_2)^2 + (h_2|s_1)^2(h_1|s_2)^2\right. \\ &\qquad \left.\left. + (s_1|s_2)^2(h_1|h_2)^2\right]\right\} \\ &- 4\left[(s_1|s_2)(h_1|h_2)\left\{(h_2|s_1)(h_1|s_2)\right.\right. \\ &\qquad \left.\left. + (h_1|s_1)(h_2|s_2)\right\} - 2(h_1|s_1)(h_2|s_2)\right. \\ &\qquad \left. \times (h_1|s_2)(h_2|s_1)\right].\end{aligned} \tag{A-22}$$

In order to check the result for the open-shell case, the formulae were specialized to the closed-shell case by setting $s_1 = s_2 = s$ and $h_1 = h_2 = h$. The expression for H_{AA} then becomes

$$\begin{aligned}H_{AA} = 2&\left[1 - (h|s)^2\right](s|H|s) + (h|H|h) \\ &+ 4\left[(h|s)^3 - (h|s)(h|H|s)\right] \\ &+ 2\left[2 - (h|s)^2\right](ss|hh) \\ &+ 2\left[3(h|s)^2 - 1\right](hs|hs) \\ &- 4(h|s)\left[(hs|ss) + (hh|hs)\right] \\ &+ (ss|ss) + (hh|hh)\end{aligned} \tag{A-23}$$

and

$$\Lambda_{AA} = \left[1 - (h|s)^2\right]^2 \tag{A-24}$$

where a factor of sixteen has been dropped in both (A-23) and (A-24).

The expression for the energy is then equivalent to

that given by Eq. (6) in Section II.

A numerical check for the closed-shell case was made by recalculating the curve for $Li^+ - H^-$ included by Slater in his discussion of Karo and Olson's calculation[54] of the LiH molecule.

Appendix B

The LCAO-MO-SCF problem consists of obtaining an approximate solution of the Schrodinger equation for electronic motion in the field of a group of fixed nuclei and a group of point ions,

$$\mathcal{H}_e \Psi_e = E_e \Psi_e \qquad \text{(B-1)}$$

where E_e is the electronic energy of the system and Ψ_e is the electronic wave function. The Hamiltonian operator is given by

$$\mathcal{H} = \sum h(1) + \sum \frac{1}{r_{ij}} \qquad \text{(B-2)}$$

where h(1) is the one electron operator which includes "nuclear attraction" terms to the point ions, and where the sum extends over all electrons.

The solution of Eq. (B-1) is found by use of the Variation Principle. The variational wave function used is a single determinant Ψ_p of M doubly-occupied molecular orbitals,

$$\Psi_p = \frac{1}{2M!} \det \phi_1(1)\alpha(1)\phi_1(2)\alpha(2) \ldots \qquad \text{(B-3)}$$
$$\ldots \phi_M(2M-1)\alpha(2M-1)\phi_M(2M)\alpha(2M)$$

where the molecular orbitals are formed from linear combinations of atomic orbitals. For a basis set of N functions,

$$\phi_r = \sum_{i}^{N} Y_{ri} \chi_i \qquad \text{(B-4)}$$

where χ_i are the Gaussian atomic orbitals and Y_{ri} are var-

iable coefficients.

Roothaan[43] has shown that the coefficients Y_{ri} can be determined by solving the eigenvalue problem

$$FY_r = \varepsilon_r GY_r \tag{B-5}$$

where Y_r is a column vector with components Y_{ri}, ε_r is the orbital energy and G is the NxN overlap matrix of the basis functions

$$G_{ij} = (\phi_i|\phi_j) \tag{B-6}$$

The NxN Fock matrix F is given by

$$F = H + 2J - K \tag{B-7}$$

where

$$H_{ij} = (\phi_i|h(1)|\phi_j) \tag{B-8}$$

$$J_{ij} = \sum_{k,l} P_{kl}(\phi_i\phi_j|\phi_k\phi_l) \tag{B-9}$$

$$K_{ij} = \sum_{k,l} P_{kl}(\phi_i\phi_k|\phi_j\phi_l) \tag{B-10}$$

and the elements of the "density matrix" are given by

$$P_{kl} = \sum_{r} Y_{rk}Y_{rl} \tag{B-11}$$

where the summation is over the occupied orbitals. The two-electron integrals are as shown in Table A-1, Appendix A, with the notation as used in Eq. (A-17). The total energy is given by

$$E = \text{trace}\left[(H + F)P\right] \tag{B-12}$$

Since the matrix $\underline{F}$ involves the values of Y_{ri}, the solution of Eq. (B-5) is found by an iterative process.

An initial estimate is made for Y and this is used to compute , J and K. These are used with H and G to find a new set of N vectors Y_r and associated orbital energies ϵ_r by solving Eq. (B-5). Of the N orbitals, M are occupied and N - M are virtual orbitals. The process is repeated until the total energy of the occupied orbitals converges within a specified limit.

This iterative method, described by Roothaan[43] can be carried out for the defect problem with the POLYATOM program[44] designed for non-empirical calculations of the properties of molecules. Those ions that are not structured in the many-body models for LiH and LiH:He are treated in the same way as the nuclei in the structured centers, with the ionic charge replacing the nuclear charge.

The program consists of three parts. The first part creates files containing lists of labels for the various one- and two-electron integrals. The symmetry properties of the one-electron functions, which are determined by the symmetry properties of the structured group of ions and by the symmetry types of the functions themselves, can be specified as input to this part of the program. No labels are created for integrals which are identically zero and labels referring to integrals related by symmetry properties are stored consecutively.

In the second part of the program, the one-electron functions themselves are fed in and the overlap, kinetic energy, nuclear attraction and electronic repulsion integrals

are evaluated. All integrals with values below a limit specified as input data are eliminated. Also calculated in this part of the program is the "nuclear repulsion" energy, which includes the electrostatic interaction of the point ions in this problem.

The third part of the program performs the SCF calculations by an indirect iterative solution of Eq. (B-5) with the limit of convergence specified as input data. The actual problem solved is[55]

$$F'U = UE \tag{B-13}$$

where

$$F' = VFV^{\dagger} \tag{B-14}$$

$$VGV^{\dagger} = I \tag{B-15}$$

and

$$Y = U^{\dagger}V \tag{B-16}$$

This method differs from the usual A-matrix method.[56]

Symmetry orbitals corresponding to irreducible representations of the symmetry group can be introduced as input to this part of the program. If this is done, the eigenvalue equation is reduced to a set of equations for each symmetry type since orbitals belonging to different representations are orthogonal. The occupancy of each symmetry type must be specified. The solution of the SCF calculation will not give the ground state energy unless the occupied orbitals correspond to the M lowest orbital energy eigenvalues.

In the output of part three, the total electronic energy, which is the energy tested for convergence, is broken down for each iteration into the one-electron energy, includ-

ing kinetic and potential, and the two-electron potential energy. The part of the one-electron potential energy which represents a "nuclear attraction" to a point ion will combine with that part of the "nuclear repulsion" energy which represents an electrostatic interaction between a point ion and a nucleus of a structured ion, to give the total interaction energy between a structured ion and a point ion. The constant total value of the "nuclear repulsion" energy found in the second part of the program is added to the total electronic energy at each iteration to give a total energy for the model. Because there is no overlap repulsive energy between point ions, this total energy has no physical meaning. It is assumed that this energy cancels in the models of LiH and LiH:He.

The coefficients Y_{ri} are given for each iteration along with the corresponding orbital energies for the final Y_{ri} values. The other matrices may also be printed out by use of the appropriate program controls.

References

1. P. O. Lowdin, Phil. Mag. Supplement 5, 1 (1956) This comprehensive review article contains reference to previous work on LiH and an extensive discussion of the quantum theory of ionic crystals.

2. C. E. Messer, A Survey Report on Lithium Hydride, U.S. Atomic Energy Commission Report # NYO-9470 (1956)

3. F. E. Pretzel, D. T. Vier, E. J. Szklarz and W. B. Lewis, Los Alamos Scientific Laboratory Report, LA 2463 (1961)

4. F. E. Pretzel and R. L. Petty, Phys. Rev. 127, 777 (1962)

5. P. C. Souers, T. A. Jolly and C. F. Cline, Lawrence Radiation Laboratory Report, UCRL-70143 Rev. I (1967)

6. P. M. S. Jones, United Kingdom Atomic Energy Authority Report, AWRE No. O-27/67 (1967)

7. B. Holt, private communication

8. M. P. Tosi, Solid State Physics 16, 1 (1964)

9. L. Dass and S. C. Saxena, J. Chem. Phys. 43 1747 (1965)

10. E. C. Baughan, Trans. Faraday Soc. 55, 736 (1959)

11. L. W. Barr and A. B. Lidiard, Vol. 10 of Physical Chemistry - an Advanced Treatise, Academic Press Part 2 of this survey article discusses the use of the classical ionic model in defect calculations and the limitations of the empirical Born-Mayer interaction.

12. E. A. Hylleraas, Zeits. Physik 63, 771 (1930)

13. S. O. Lundquist, Arkiv Fysik 8, 177 (1954)

14. A. Morita and K. Takahashi, Prog. Theor. Phys. 19, 257, (1958)

15. R. P. Hurst, Phys. Rev. 114, 746 (1959)

16. C. R. Fischer, S. W. Harrison, R. D. Hatcher and W. D. Wilson, Bull. Am. Phys. Soc. 13, 500 (1968)

17. C. R. Fischer, T. A. Dellin, S. W. Harrison, R. D. Hatcher and W. D. Wilson, Phys. Rev. 1, 870 (1970)

18. W. D. Wilson and R. A. Johnson, Phys. Rev. [illegible] (1970)

19. T. A. Dellin, G. J. Dienes, C. R. Fischer, R. D. Hatcher and W. D. Wilson, Phys. Rev. B 1 1745 (1970)

20. R. D. Hatcher and G. J. Dienes, Phys. Rev. 124, 126 (1961)

21. W. D. Wilson, R. D. Hatcher, R. Smoluchowski and G. J. Dienes, Phys. Rev. 184, 844 (1969)

22. S. S. Jaswal and M. E. Streifler, Bull. Amer. Phys. Soc. 16, 438 (1969)

23. S. W. Harrison and C. R. Fischer, Bull. Amer. Phys. Soc. 14, 612 (1969)

24. L. Pauling, Proc. Roy. Soc. A114, 181 (1927)

25. P. O. Lowdin, Phys. Rev. 97, 1474 (1955)

26. J. S. Slater, Quantum Theory of Molecules and Solids Vol. I, McGraw-Hill Book Company, Inc. New York, 1963 p. 292.

27. F. J. Corbato and A. C. Switendick in Methods of Computational Physics Vol. II, Academic Press (1963)

28. The Hartree-Fock functions for the H^- ion were supplied by Drs. A. W. Weiss and H. D. Cohen. The Li^+ functions were taken from: Roothaan, Sacks and Weiss, Rev. Mod. Phys. 32 186 (1960)

29. O. L. Anderson, J. Phys. Chem. Solids 27, 547 (1966)

30. D. R. Stephans and E. M. Lilley, J. Appl. Phys. 39, 177 (1968)

31. R. Weil and A. W. Lawson, J. Chem. Phys. 37, 2370 (1962)

32. F. Seitz, The Modern Theory of Solids, McGraw-Hill Book Company, New York 1940

33. K. G. Subhadra and D. B. Sirdeshmukh, J. Appl. Phys. 40, 2357 (1969)

34. M. Born, J. Chem. Phys. 7, 591 (1939); Proc. Cambridge Phil. Soc. 36, 160 (1940)

35. A. Westin, I. Waller and S. O. Lundquist, Arkiv fur Fysik 22, 371 (1962)

36. A. A. Abrahamson, Phys. Rev. 178, 76 (1969)

37. J. Tessman, A. Kahn and W. Shockley, Phys. Rev. 92, 890 (1953)

38. Y. Varshni and R. Shukla, Rev. Mod. Phys. 35, 130 (1963)

39. P. T. Wedepohl, Solid State Commun. 4, 479 (1966)

40. S. S. Jaswal and J. R. Hardy, Phys. Rev. 171, 1090 (1968)

41. S. S. Jaswal and M. E. Streifler, Phys. Rev. (1970)

42. S. S. Jaswal and P. Schulze, Bull. Amer. Phys. Soc. 15, 389 (1970)

43. C. C. J. Roothaan, Rev. Mod. Phys. 23, 69 (1951)

44. I. G. Csizamadia, H. C. Harrison, J. W. Moskowitz and B. T. Sutcliffe, Theoret. Chim. Acta. (Berlin) 6, 191 (1966)

45. I. G. Csizamadia, Jour. Chem. Phys. 44, 1849 (1966)

46. S. Huzinaga, Jour. Chem. Phys. 42, 1239 (1965)

47. J. P. Chesick, S. J. Frazer and J. W. Linnett, Trans. Faraday Soc. 64, 257 (1968)

48. A. Froman and P. O. Lowdin, J. Phys. Chem. Solids 23, 75 (1962)

49. The program DENPLOT was written by P. Mattern and P. J. Kemmey of the Brookhaven National Laboratory and used for this problem with minor revisions.

50. R. M. Sternheimer, Phys. Rev. 107, 1565 (1957)

51. P. O. Lowdin, Phys. Rev. 90, 120 (1953)

52. P. Rosen, J. Appl. Phys. 18, 1182 (1950)

53. J. S. Slater, op. cit. p. 139

54. A. M. Karo and A. R. Olson, J. Chem. Phys. 30, 1232 (1959)

55. I. G. Csizmadia, M. C. Harrison, J. W. Moskowitz, S. Seung, B. T. Sutcliffe and M. P. Barnett, Technical Note No. 36, Cooperative Computing Laboratory, Massachusetts Institute of Technology

56. R. K. Nesbet, Rev. Mod. Phys. 35, 552 (1963)

Vita

Shirley W. Harrison

Education

Columbia University Graduate Faculties
A. M. Physics, June '46

Barnard College, Columbia University
A. B. Mathematics and Physics, June '44

Fellowships

New York State Regents College Teaching Fellowship, Sept. '68 - June '69

City University of New York
NASA Traineeship, Sept. '65 - June '69

Research

Brookhaven National Laboratory
Guest Junior Research Associate
May '68 to present

Queens College, City University of New York
Research Assistant, Sept. '68 - Jan. '69

General Telephone and Electronics Laboratories (formerly Sylvania Research Laboratories), Research Physicist,
July '46 - Aug. '61

E. I. duPont de Nemours and Company
Research Laboratories
Junior Physicist, Summer '44

Teaching

New College of Hofstra University
Teaching Fellow in the Physical Sciences
Spring '70

Queens College, City University of New York
Lecturer in Physics, Jan. '69 - Jan. '70

Connecticut College for Women
Lecturer in Physics, Summer '45

Barnard College, Columbia University
Lecturer in Mathematics and Physics,
Sept. '44 - June '45